

A System Identification Approach to Dynamically
Modeling and Understanding Physical Activity Behaviors

by

Gustavo Mesel Lobo Seixas

A Thesis Presented in Partial Fulfillment
of the Requirements for the Degree
Master of Science

Approved November 2016 by the
Graduate Supervisory Committee:

Daniel E. Rivera, Chair
Matthew M. Peet
Terry L. Alford

ARIZONA STATE UNIVERSITY

December 2016

©2016 Gustavo Mesel Lobo Seixas

All Rights Reserved

ABSTRACT

The lack of healthy behaviors - such as physical activity and balanced diet - in modern society is responsible for a large number of diseases and high mortality rates in the world. Adaptive behavioral interventions have been suggested as a way to promote sustained behavioral changes to address these issues. These adaptive interventions can be modeled as closed-loop control systems, and thus applying control systems engineering and system identification principles to behavioral settings might provide a novel way of improving the quality of such interventions.

Good understanding of the dynamic processes involved in behavioral experiments is a fundamental step in order to design such interventions with control systems ideas. In the present work, two different behavioral experiments were analyzed under the light of system identification principles and modelled as dynamic systems.

In the first study, data gathered over the course of four days served as the basis for ARX modeling of the relationship between psychological constructs (negative affect and self-efficacy) and the intensity of physical activity. The identified models suggest that this behavioral process happens with self-regulation, and that the relationship between negative affect and self-efficacy is represented by a second order underdamped system with negative gain, while the relationship between self-efficacy and physical activity level is an overdamped second order system with positive gain.

In the second study, which consisted of single-bouts of intense physical activity, the relation between a more complex set of behavioral variables was identified as a semi-physical model, with a theoretical set of system equations derived from behavioral theory. With a prescribed set of physical activity intensities, it was found that less fit participants were able to get higher increases in affective state, and that self-regulation processes are also involved in the system.

Dedicated to Eli, who above all encouraged me to be where I am.

ACKNOWLEDGMENTS

First of all, I would like to express my gratitude to my research advisor, Dr. Daniel E. Rivera. Not only is he an excellent professor, having taught me two important control systems courses, but also his patience, dedication, and knowledge were fundamental to my development and to the completion of this work. Prior to taking his courses and joining his research group in 2015, my background in control systems engineering was very lacking; all the knowledge I have gathered and the skills I have now are all thanks to him.

I would also to thank Dr. Matthew Peet and Dr. Terry Alford for serving on my thesis committee, offering their time and support for the improvement and expansion of this work.

I wish to acknowledge Dr. Genevieve Dunton (Institute for Health Promotion & Disease Prevention Research, USC) and Dr. John Bartholomew (Department of Kinesiology and Health Education, UT Austin) for their crucial collaboration. Due to the substantial inter-disciplinary nature of this research, this work would not have been possible without the data sets they have provided and the discussions, interpretations, and advice they have given.

My thanks to all the colleagues in the Control Systems Engineering Laboratory at ASU, past and present: Dr. César Martin Moreno, Mohammad Freigoun, Penghong Guo, and Alicia Magann. Not only did they provided assistance with the research but their presence also turned the lab a pleasant and fun environment. This gratitude also applies to Dr. Paulo Lopes dos Santos from Universidade do Porto (Portugal) for his friendship and help.

I would also like to acknowledge all my family and friends, both distant and near,

for all their support and encouragement. Without them, my time here would have been more difficult.

Lastly, I would like to acknowledge CAPES and IIE for their collaborative support and scholarship, without which my work here would not have been possible. The opinions expressed in this document are the author's own and do not necessarily reflect the views of the organizations that provided funds supporting my training, research, or resulting publication.

TABLE OF CONTENTS

	Page
LIST OF TABLES	vii
LIST OF FIGURES	viii
CHAPTER	
1 INTRODUCTION	1
1.1 Thesis Outline	6
1.2 Justification	7
1.3 System Identification Principles	8
1.4 Prediction Error Methods	10
1.5 Semi-Physical Modeling.....	14
1.6 Fluid Analogies	15
1.7 Model Validation	19
2 BLACK-BOX SYSTEM IDENTIFICATION IN OBSERVATIONAL BEHAVIORAL STUDY	23
2.1 Overview	23
2.2 Data Collection Overview	25
2.3 Participants and Recruitment	27
2.4 Data Analysis and Pre-Treatment	29
2.5 ARX Modeling	33
2.6 Model Validation	36
2.7 Results and Discussion.....	38
2.7.1 All Participants - General Considerations	40
2.7.2 Age Aggregation	45
2.7.3 Gender Aggregation	47

CHAPTER	Page
2.7.4 BMI Category Aggregation	49
2.8 Control Systems Perspectives	51
3 SEMI-PHYSICAL MODELING OF BEHAVIORAL SYSTEM IN SINGLE-BOU T PHYSICAL ACTIVITY	54
3.1 Overview	54
3.2 Data Analysis and Pre-Treatment	58
3.3 Fluid Analogy and Mathematical Representation	65
3.4 Grey-Box Modeling	69
3.5 Results and Discussion	74
4 CONCLUSIONS	83
4.1 Future Work	85
REFERENCES	88
APPENDIX	
A ESTIMATED ARX PARAMETERS FOR DYNAMIC SYSTEMS IDEN- TIFIED IN CHAPTER 2	94
B GREY-BOX MODELING CONSIDERATIONS FOR SYSTEMS IDEN- TIFIED IN CHAPTER 3	97

LIST OF TABLES

Table	Page
1 Common PEM Model Structures	14
2 ARX Structure, Estimation-Validation Sets, and Goodness-Of-Fit for All Cohorts for First Identification Problem (NA as Input, SE as Output)	39
3 ARX Structure, Estimation-Validation Sets, and Goodness-Of-Fit for All Cohorts for Second Identification Problem (SE as Input, MVPA as Output) .	40
4 Notation for Input and Output Signals in Fluid Analogy for Studied Behavioral System	67
5 Goodness-Of-Fit for Simulated Systems for Each Cohort	76
6 Estimated Parameters for Semi-Physical Modeling	77
7 Estimated ARX Parameters	95
8 Estimated ARX Parameters (Cont.)	96
9 Initial Parameters for Grey-Box Simulation	98
10 Goodness-Of-Fit for Representative Simulations Above	100

LIST OF FIGURES

Figure	Page
1 Structural Path Diagram for TPB (Navarro-Barrientos <i>Et Al.</i> , 2011).....	16
2 Proposed Fluid Analogy for TPB Corresponding to Diagram Shown in Figure 1 (Navarro-Barrientos <i>Et Al.</i> , 2011).	17
3 Open-Loop Behavioral Model from Social Cognitive Theory	24
4 Simplified Open-Loop Behavioral Model	25
5 Representative Time Series Used Prior to Identification - All Participants, Day 1	32
6 Representative System Identification Toolbox App Window.....	34
7 Step Response from NA to SE for All Participants	41
8 Step Response from SE to MVPA for All Participants	41
9 Step Response from SE to MVPA for All Participants Including 95% Confi- dence Intervals	44
10 Step Response from NA to SE for Participants with Age Less than Median (Blue, Solid) and Age Higher than Median (Red, Dash-Dotted)	45
11 Step Response from SE to MVPA for Participants with Age Less than Median (Blue, Solid) and Age Higher than Median (Red, Dash-Dotted)	46
12 Step Response from NA to SE for Male (Blue, Solid) and Female (Red, Dash-Dotted) Participants	47
13 Step Response from SE to MVPA for Male (Blue, Solid) and Female (Red, Dash-Dotted) Participants	48
14 Step Response from NA to SE for Underweight / Normal Participants (Blue, Solid) and Overweight / Obese Participants (Red, Dash-Dotted)	49

Figure	Page
15 Step Response from NA to SE for Underweight / Normal Participants (Blue, Solid) and Overweight / Obese Participants (Red, Dash-Dotted)	50
16 Closed-Loop Behavioral Dynamics	51
17 Behavioral Self-Regulatory Process	52
18 Fluid Analogy for Behavioral Self-Regulation	53
19 Initially Proposed Path Diagram for Single Exercise Bout	56
20 Proposed Path Diagram for Single Exercise Bout	57
21 Time Series for Representative Participant after Linear Interpolation	59
22 FAS Signal for Third Cohort Before (Left) and After (Right) Pre-Treatment .	60
23 Time Series for Participants with Reported Pride ≤ 3	61
24 Time Series for Participants with Reported Pride = 4	61
25 Time Series for Participants with Reported Pride = 5	62
26 Time Series for All Participants	62
27 Revised Path Diagram with Addition of "Experiment Begins" Exogenous Input	64
28 Fluid Analogy for the Proposed Behavioral Diagram Path	66
29 Simulated Outputs (Blue, Dashed) versus Experimental Outputs (Red, Dash-Dotted) for First Cohort (Pride ≤ 3).	75
30 Simulated Outputs (Blue, Dashed) versus Experimental Outputs (Red, Dash-Dotted) for Second Cohort (Pride = 4).	75
31 Simulated Outputs (Blue, Dashed) versus Experimental Outputs (Red, Dash-Dotted) for Third Cohort (Pride = 5).	76
32 Unit Step Responses for First Cohort (Pride ≤ 3)	79
33 Unit Step Responses for Second Cohort (Pride = 4)	80
34 Unit Step Responses for Second Cohort (Pride = 4), without FS Response ..	80

Figure	Page
35 Unit Step Responses for Third Cohort (Pride = 5), without FS Response	81
36 Simulated Outputs(Blue, Dashed) versus Experimental Outputs (Red, Dash-Dotted) for First Cohort (Pride ≤ 3) for Diagram in Figure 18.	99
37 Simulated Outputs(Blue, Dashed) versus Experimental Outputs (Red, Dash-Dotted) for Third Cohort (Pride = 5) for Diagram in Figure 25.	99

Chapter 1

INTRODUCTION

In modern society, problems and mortality caused by behavioral issues are of major concern. It is well understood that physical activity is vital in the prevention of chronic diseases (Schroeder, 2007); however, the lack of healthy behaviors amongst many people is still a common problem. Physical inactivity, poor diet, and tobacco use contribute to major chronic diseases, being responsible for more than 50% of preventable deaths (Heckler *et al.*, 2013). The World Health Organization states that, in 2014, 39% of adults were overweight, and 13% obese (World Health Organization, 2016).

For those reasons, it is clear that any research or study aiming at promoting healthy behaviors is of fundamental importance to society. One of the solutions that has been widely proposed and studied are behavioral interventions, which, if done properly, can cause sustained lifestyle changes in the participants, promoting healthy habits like improved diet and increased physical activity levels (Navarro-Barrientos *et al.*, 2011).

Most behavioral interventions traditionally are fixed interventions. In these, the dosage of intervention components (e.g., prescription of physical activity types, intensities, and durations) are the same for all participants throughout the entire duration of the intervention (Collins *et al.*, 2004; Rivera *et al.*, 2007). There have been many criticisms about traditional health behavior theories and models because of their inability to explain behavioral processes that happens in more frequent scales, focusing

instead on limited occurrence (longer time-scale) behaviors (Noar and ZimmermVan, 2005).

With modern improvements in technology and data-gathering capabilities, so-called adaptive interventions have been increasingly studied for the context of promoting lasting behavioral changes. Unlike the fixed interventions, the goal of an adaptive intervention is to constantly adjust dosages or components throughout the intervention, adapting it to best suit the participant's needs (Collins *et al.*, 2004). In this manner, novel research has compared such adaptive intervention with closed-loop feedback control systems (Rivera *et al.*, 2007), since those are defined by constant, or frequent, adjustments of manipulated variables based on measurements of controlled variables. Thus, control systems engineering – combining system identification techniques and controller design principles – might prove to be useful tools for modeling behavioral systems and designing interventions, respectively.

Dynamical systems and control represent well-known engineering fields of study, with diverse practical applications in chemical processing, robotics, mechanical engineering, aerospace systems, electronics, amongst others. Control systems engineering is the study and application of mathematical and computational tools and techniques with the goals of analyzing, manipulating, controlling, and optimizing a system (whether it is chemical, mechanical, electronic, etc.). This control is made through the manipulation of inputs $u(t)$ – or manipulated variables – with the goals of reaching desired levels (also known as setpoint) for some variables that cannot be directly manipulated – called outputs $y(t)$ – even in the presence of disturbances (which can be thought of as undesired, non-manipulated, and/or non-measurable inputs). The goals of controlling processes and systems are many, including optimized productivity

and/or efficiency, cost reduction, ensuring product quality, and increase in operational safety (Ogunnaike and Ray, 1994).

In order for a system or plant control to be effectively implemented, it is necessary, or at least extremely desirable, that dynamical structural mathematical relations between the many variables that compose the system are known. Dynamic systems modeling allows the process to be characterized by a transient response between the inputs and outputs (which can be defined even outside a controller's perspective – inputs are either the manipulated inputs or disturbances, while outputs are the measurement of interest in terms of modeling and prediction). Dynamic systems are usually represented as a set of ordinary differential equations (for continuous-time systems) or difference equations (for discrete-time), and/or represented by a set of transfer functions that relate each system output to one or more inputs or disturbances (Ogunnaike and Ray, 1994).

The advantages of dynamically modeling systems and processes lie in the fact that the causal relationship between variables can be represented in the model. In other words, it is possible to analyze how a specified change in any input variable affects the outputs, not only in terms of final stationary net changes but also in terms of speed of response (how slow or fast the output settles) and shape of response (i.e., whether the response is smooth or oscillatory, presence or absence of inverse response and/or overshoot) (Ogunnaike and Ray, 1994; Franklin *et al.*, 2006).

Sometimes, the equations or transfer functions that represent a dynamic model can be readily obtained through first principles (such as material or energy balances). However, the most common case is that in which the studied systems are so complex that a mere theoretical analysis proves incapable of modeling all the relations between the variables. For this reason, many dynamic systems are currently modeled with

system identification techniques, which stands for the computational and statistical tools that allow for dynamical equations and/or transfer functions that model a system be obtained through measured input-output data (Ljung, 2001). The methods and tools provided by system identification includes initial experiment design (in data collection phases) – in order to obtain a data set that allows for meaningful identification; data treatment and preprocessing; model structure selection or determination; parameters estimation; and model validation (Dunton *et al.*, 2015). The advantages of using system identification can be found in the ability of predicting and/or modeling statistically significant systems without the need of an internal theoretical system’s knowledge (although such knowledge can greatly improve the quality of the obtained models). For this reason, system identification plays a major role in control systems engineering (Ogunnaike and Ray, 1994).

As previously described, control systems engineering already finds wide applications in the fields of engineering and technology. However, with recent technological and computational advances, the capacity to study and apply such controls and system identification concepts to less conventional fields of study is increasing, such as medicine (Wellstead *et al.*, 2008; Ahn *et al.*, 2006), supply chain optimization (Wang and Rivera, 2008; Schwartz *et al.*, 2006; Nandola and Rivera, 2013), and economics (Neck, 2009). The central idea is similar: any system that can be mathematically modeled as a set of inputs, outputs, and disturbances with inter-relations can, in theory, benefit from dynamic modeling and control techniques, so that transient responses can be analyzed and, with proper controlling, faster, safer, and/or more efficient levels of specified variables can be achieved.

Of particular interest, one such less conventional (in relation to traditional control systems engineering) field of study is behavioral sciences. Recent inter-disciplinary

research has been pursued regarding the implementation of controller design and system identification principles to understand, model, control and/or optimize behavioral problems (Carver and Scheier, 2002; Martín Moreno, 2016; Navarro-Barrientos *et al.*, 2011; Rivera *et al.*, 2007; Dong *et al.*, 2013, 2012; Vanderwater and Davison, 2009, 2012; Davison *et al.*, 2011; Timms, 2014; Dunton *et al.*, 2015). Behavioral processes can be modeled as dynamical systems that describe the relationships and interconnections between psychological and physiological variables and behavioral components. As such, as mentioned before, an adaptive intervention share similarities with closed-loop control systems (mostly feedback controllers). In Martín Moreno (2016), a design for a closed-loop (adaptive) behavioral intervention using controller principles is proposed.

The benefits of using control systems concepts for behavioral health systems are apparent. A participant in a behavioral experiment might present optimal levels of a certain studied behavior according to the many inputs and disturbances that composes the system, making the study and manipulation of these desirable. As a hypothetical example regarding physical activity behaviors, participants with lower physical conditioning might get demotivated more easily in case the level or intensity of a physical activity prescription is too elevated, and that demotivation might hamper the performance in that activity, negatively influencing the result. On the other hand, very light physical activity prescriptions might make a participant take longer to visualize improvements in associated outcomes (for example, weight loss), and that might demotivate the participant, which again, could influence negatively the behavior. In this hypothetical example, physical activity could be modeled as a dynamic system with inputs and outputs, including activity prescription levels, outcomes, outcome expectancies and motivation.

1.1 Thesis Outline

In this research, two different case studies of behavioral processes, both concerning physical activity, are analyzed through the lens of system identification. Input/output data for these experiments are used in conjunction with behavioral theories to obtain dynamic models through different system identifications techniques.

This thesis is structured in the following way:

Chapter 1 introduces the main ideas and also explains the importance of improving health interventions and how system interventions and how system identification can be used to study behavioral processes. This chapter also explains the basic mathematical principles of system identification.

Chapter 2 is the first case study, in which participant behavioral data was collected in the course of four days and then used to obtain dynamic models - a model that relates mood (negative affect) and self-efficacy, and another model that relates self-efficacy to moderate-to-vigorous physical activity (MVPA) - through ARX modeling. Modeling results show negative oscillatory response for the first system, and positive smooth response for the second. The results suggests the presence of self-regulatory behavioral processes for the participants.

Chapter 3 describes the second study. Participants performed single-bouts of exercise and their physiological (heart rate) and psychological (rate of perceived exertion, felt arousal scale, and feeling scale) constructs were measured. Based on behavioral theories, a suggested structural path diagram was mathematically analysed through a fluid analogy. Semi-physical identification was carried based on the experimental data and the theoretical model, resulting in estimated parameters for the dynamic relations that described the system.

Finally, Chapter 4 concludes this thesis and presents suggestions for improvements on this work.

1.2 Justification

The vast number of chronic diseases, health issues, and deaths caused by behavioral problems (as in, the lack of healthy behaviors) in modern society justify the need for research that improve the design and efficacy of behavioral interventions, which aims to promote sustained lifestyle changes in individuals. Optimally performed interventions have the potential of reducing the amount of preventable deaths and diseases caused by behavioral risk factors such as physical inactivity and poor diets

Control systems engineering represent a novel approach to handling such behavioral health problems, with one of the ultimate goals being applying controller design principles to adaptive interventions. However, as in any control system design, this requires good understanding of the dynamical interrelations between the many variables that comprises the behavioral system. For that purpose, a good understanding of system identification principles and how to apply them become a necessity for the design of adaptive intervention as a control system.

System identification is already a broad discipline, with many different tools and techniques that can be applied in different scenarios. For many traditional engineering and technology applications, which have benefited from control systems principles for years, the problem of finding statistically significant dynamic models through system identification techniques is not trivial; that is even more true for this novel research applying system identification in behavioral sciences.

For that reason, any attempt to understand how behavioral problems can be

modeled as dynamic systems, to examine how system identification techniques might be used in such behavioral processes, and to analyze and interpret dynamic models obtained through system identification, is a necessary step towards improving the quality of adaptive interventions based on control designs. With a better grasp of the dynamics of behavioral systems, not only can these processes be better understood, but also better performing adaptive interventions can be designed, which represents a significant improvement in behavioral health studies.

1.3 System Identification Principles

As described previously, the goal of system identification is to obtain useful dynamic models that allow for a system's prediction, simulation, and/or control. The techniques used to obtain such dynamic structures are varied in numbers and scope. System identification is a very broad problem, and thus there are different ways to approach the modeling a system, each one having their advantages and drawbacks (Ljung, 1999).

One way to categorize methods to model dynamic systems is based on the requirement of using mathematical principles and/or collected data. In that regard, there are three different types of models:

White-box models are those obtained exclusively through first-principles (such as conservation of energy or momentum) and/or theoretical knowledge and information about the system in question. Thus, even though it is possible to get dynamic model through this method, it is outside the scope of the system identification discipline, since it does not utilize data in the modeling. White-box models are based on *a priori* knowledge of the system, but it has a major disadvantage in that process complexities,

unknown dynamics, and random effects might severely weaken the model (Bohlin, 2006).

Black-box models, on the other hand, lack prior information about the system and is based almost solely on measured input/output data. This type of modeling is widely used because many real world processes and systems are inherently complex, and/or because these system's construction are unknown, in a way that physical insight has no real value or cannot be used properly. When that's the case, standard black-box models can be used, that are empirically known to model well a great number of dynamic systems (Ljung, 2001). However, these type of models might show poor reproducibility, as in significantly different model structures might be obtained when repeating the same experiments with only minor experimental modifications. Also, the models obtained through black-box identification are not always easily interpreted – the model can describe parameters and structures which might lack in physical significance (Bohlin, 2006).

Finally, combining the purely theoretical physical/structural knowledge with statistical tools applied to gathered input/output data results in the so called grey-box models (also called semi-physical models). There are a wide range of different grey-box models, including those that are a theoretical model with some parameter values determined from data, those almost exclusively modeled from experimental data but with only a small fraction based on theoretical structures, and all in-between (Whiten, 2013). Semi-physical modeling combines the advantages of prior internal system knowledge with statistical data analysis, but as with any other modeling strategy, has its own drawbacks. Grey-box identification tends to be harder to perform in a numerical sense, presenting problems such as hard computing, great need for interactivity, and higher chance of numeric failures (Bohlin, 2006).

Each of the behavioral experiments studied in this research was modeled using one of the techniques mentioned above (excluding white-box modeling, since it deviates from the scope of system identification). In the the first study (Chapter 2), classic prediction-error methods were used for estimating model parameters only from experimental data, characterizing the steps as black-box identification; in the second study (Chapter 3), a previously postulated behavioral diagram was described in mathematical terms using a fluid analogy, resulting in a system of differential equations in which parameters were obtained through grey-box estimation.

1.4 Prediction Error Methods

One of the system identification methods used in this research is the classical sampled-data prediction error models. This process involves fitting the system into a user-defined model structure and order, and then numerically estimating the chosen structure’s parameters by minimizing the prediction errors. This is made in a way that, at every time point, current and previous data points are used to estimate “step-ahead” (beyond that time point) predictors (Ljung, 1999). The basic ideas behind the prediction error methods are described in Ljung (2001). First, the model is described as a predictor of the output:

$$\hat{y}_m(t|t-1) = f(Z^{t-1}) \tag{1.1}$$

Where \hat{y}_m is the one-step ahead prediction of the output, f is an arbitrary function, and $Z^N = \{u(1), y(1), u(2), y(2), \dots, u(N), y(N)\}$ is a vector containing the measurement of all current and past experimental data points up to time instance

N . Equation 1.1 represents the idea of obtaining a one-step ahead prediction of the output as a function of current and past data (both inputs and outputs).

Then, these step-ahead predictors are parametrized, or in other words, written as a function of a parameter vector, represented by θ :

$$\hat{y}(t|\theta) = f(Z^{t-1}, \theta) \quad (1.2)$$

Based on the model parametrization and the data set, the parameters θ are estimated such that the difference between the predictors and the actual output measurements – defined as the prediction error, $e(t)$, are minimized:

$$e(t) = y(t) - \hat{y}(t|t-1) \quad (1.3)$$

The minimization problem can be stated as:

$$\hat{\theta}_N = \arg \min_{\theta} V_N(\theta) \quad (1.4)$$

$$V_N(\theta) = \sum_{t=1}^N \ell(y(t) - f(Z^{t-1}, \theta)) \quad (1.5)$$

Where Equation 1.4 means that the estimated parameters ($\hat{\theta}_N$) are the ones that minimizes the function V_N . In Equation 1.5, ℓ represents a suitable distance function (Ljung, 2001). For example, ℓ could be a quadratic norm (Ljung, 1999):

$$\ell(\varepsilon) = \frac{1}{2} \varepsilon^2 \quad (1.6)$$

There are many distinct ways of approaching a prediction error method problem, these include choices of predictor function f , the minimization procedure $\ell(e)$, and even a possible pre-filtering of the predictor error vector. The parametrization function,

f , can be Linear Time Invariant (LTI), meaning that the relation between predictors, parameters and measured data are linear, and the parameters are time-invariant; more complicated model structures might present time-invariant parameters and/or non-linear expressions (Ljung, 2001).

When opting for identifying a system using a LTI model, which is a common first attempt in many identification problems, Equation 1.2 can be written as:

$$\begin{aligned} f(Z^{t-1}, \theta) &= W_y(q, \theta)y(t) + W_u(q, \theta)u(t) = \\ &= \sum_{k=1}^{t-1} w_y(k)y(t-k) + \sum_{k=1}^{t-1} w_u(k)u(t-k) \end{aligned} \quad (1.7)$$

When a linear time-invariant model is assumed for identification purposes, the relation between output and input becomes:

$$y(t) = G(q, \theta)u(t - n_k) + H(q, \theta)e(t) \quad (1.8)$$

Where $e(t)$ is an unpredictable white-noise, and n_k is the order of the input data time delay. $G(q, \theta)$ and $H(q, \theta)$ are rational transfer functions containing the parameters. This means that there are a number of different possibilities for prediction error models structures, depending on the rational functions used. The general family of models is (Ljung, 1999):

$$A(q)y(t) = \frac{B(q)}{F(q)}u(t - n_k) + \frac{C(q)}{D(q)}e(t) \quad (1.9)$$

$$\begin{aligned}
A(q) &= 1 + a_1q^{-1} + \cdots + a_{n_a}q^{-n_a} \\
B(q) &= b_1 + b_2q^{-1} + \cdots + b_{n_b}q^{-n_b+1} \\
C(q) &= 1 + c_1q^{-1} + \cdots + c_{n_c}q^{-n_c} \\
D(q) &= 1 + d_1q^{-1} + \cdots + d_{n_d}q^{-n_d} \\
F(q) &= 1 + f_1q^{-1} + \cdots + f_{n_f}q^{-n_f}
\end{aligned} \tag{1.10}$$

Where q is the shift operator in continuous time, and the model parameters are $[a_1, \dots, a_{n_a}, b_1, \dots, b_{n_b}, c_1, \dots, c_{n_c}, d_1, \dots, d_{n_d}, f_1, \dots, f_{n_f}]$. For this most general class of LTI prediction error models, Equations 1.9 and 1.10 are related by:

$$\begin{aligned}
G(q, \theta) &= \frac{B(q)}{A(q)F(q)}q^{-n_k} \\
H(q, \theta) &= \frac{C(q)}{A(q)D(q)}
\end{aligned} \tag{1.11}$$

Not all of these polynomial transfer functions (denoted by $A(q)$, $B(q)$, $C(q)$, $D(q)$, $F(q)$) need to be used in the model; if that's the case, a value of 1 is assigned to the entire polynomial. This means that, from the general class of PEM, there are many possibilities of model structures that can be used. However, a few of these combinations prove to be more popular models due to being successfully used in many identification problems. These are:

Table 1. Common PEM Model Structures

Method	$G(q, \theta)$	$H(q, \theta)$
ARX	$\frac{B(q)}{A(q)}q^{-n_k}$	$\frac{1}{A(q)}$
ARMAX	$\frac{B(q)}{A(q)}q^{-n_k}$	$\frac{C(q)}{A(q)}$
FIR	$B(q)q^{-n_k}$	1
Box-Jenkins	$\frac{B(q)}{F(q)}q^{-n_k}$	$\frac{C(q)}{D(q)}$
Output Error	$\frac{B(q)}{F(q)}q^{-n_k}$	1

Some advantages of these prediction error methods include its capacity to be applied to a great number of different model parametrization and its ability to model closed-loop systems. Although it is not a perfect methodology, it is widely used in system identification problems (Ljung, 2001).

1.5 Semi-Physical Modeling

Another way to perform system identification is through the use of grey-box, or semi-physical, models. With this approach, a system that has an already partially determined dynamics (obtained through theoretical internal knowledge) can be completed by fitting into measured input-output data, combining aspects of white-box and black-box modeling. Many times, a mathematical model obtained through first principles (white-box model) needs to be simplified, or the model cannot capture all the interactions due to a system's complexity. In that case, combining theoretical knowledge with data fitting brings a number of advantages, such as the estimation of model parameters that yield physical significance (Hauth, 2008).

Unlike black-box modeling, it is not necessary to assume an arbitrary model structure (such as ARX) during semi-physical modeling - the model structure is already determined by the set of differential equations and/or transfer functions

known *a priori*, so the step of determining an arbitrary structure type and order does not take place in grey-box identification. That is not to say that investigating a model structure and/or order is impossible. Sometimes, the model structure obtained by theoretical knowledge might be incomplete, or some parts of it might be wrong. In these cases, the identification procedure might involve iteratively making alterations in the model in order to search for better models.

Grey box identification might be performed for linear or nonlinear systems. Linear identification procedures revolve around searching for parameters that minimize a determined loss function, similar to the prediction error method. Different parameter search methods exist that can be used to perform this estimation, such as the Gauss-Newton algorithm or the Levenberg-Marquardt method (MathWorks, 2016b).

1.6 Fluid Analogies

Behavioral models are not usually quantitatively interpreted in the same way that a physical system is. Even when a given behavioral system is presented as a structure diagram, a set of differential equations, state space, transfer functions, or any other mathematical representation of the dynamics is not promptly obtained. One possible way to obtain this mathematical representation is through a fluid analogy, such as seen in Navarro-Barrientos *et al.* (2011) and Schwartz *et al.* (2006). This is a way to convert the representation of a behavioral structural diagram into a set of inventory tanks with flows and valves, through which it is much easier to obtain dynamic mathematical relations.

In Martín Moreno (2016), the concept of fluid analogy is illustrated by applying it to the Theory of Planned Behavior (TPB) (Ajzen and Madden, 1986). TPB is a be-

havioral theory that has been widely used to explain behaviors in many situations, including physical activity (Godin *et al.*, 1993; Norman *et al.*, 2000; Symons Downs and Hausenblas, 2005). The TPB states that a person's intention is a good indicator or predictor of his or her readiness to engage the studied behavior, and that intention is shaped by the person's attitude towards the behaviour, the perceived social incentive or pressure to perform the behavior (Subjective Norm), and how the person believes he or she can engage the behavior (Perceived Behavioral Control) (Ajzen and Madden, 1986).

A path diagram and mathematical model of this behavioral theory can be obtained by a technique called Structure Equation Modeling (SEM) (Bollen, 1989). The result of this modeling is the path diagram presented in Figure 1.

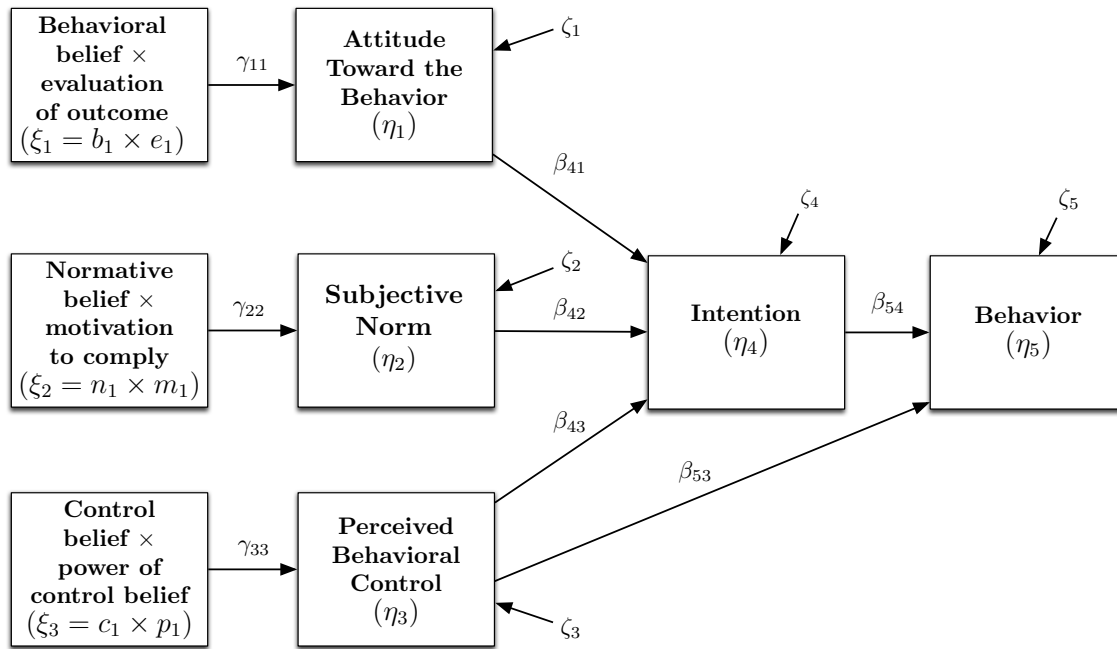


Figure 1. Structural Path Diagram for TPB (Navarro-Barrientos *et al.*, 2011).

The diagram in Figure 1 shows the relations between the constructs for this

behavioral theory (Attitude Towards Behavior; Subjective Norm; PBC; Intention; and Behavior) described in a mathematical manner, with (qualitatively explaining) η_i being the quantity of a particular construct i , β_{ij} the amount of influence that construct j exerts on construct i , ζ_i representing a random, unpredictable change to construct i , ε_i represents an exogenous variable influencing the initial constructs, and γ_{ij} being the amount of such influence.

The structural path diagram fails to show the dynamic mathematical relations between the constructs. That is how the fluid analogy becomes a useful technique; assuming a linear system, the dynamics represented as a set of inventory tanks and flows are presented in Figure 2.

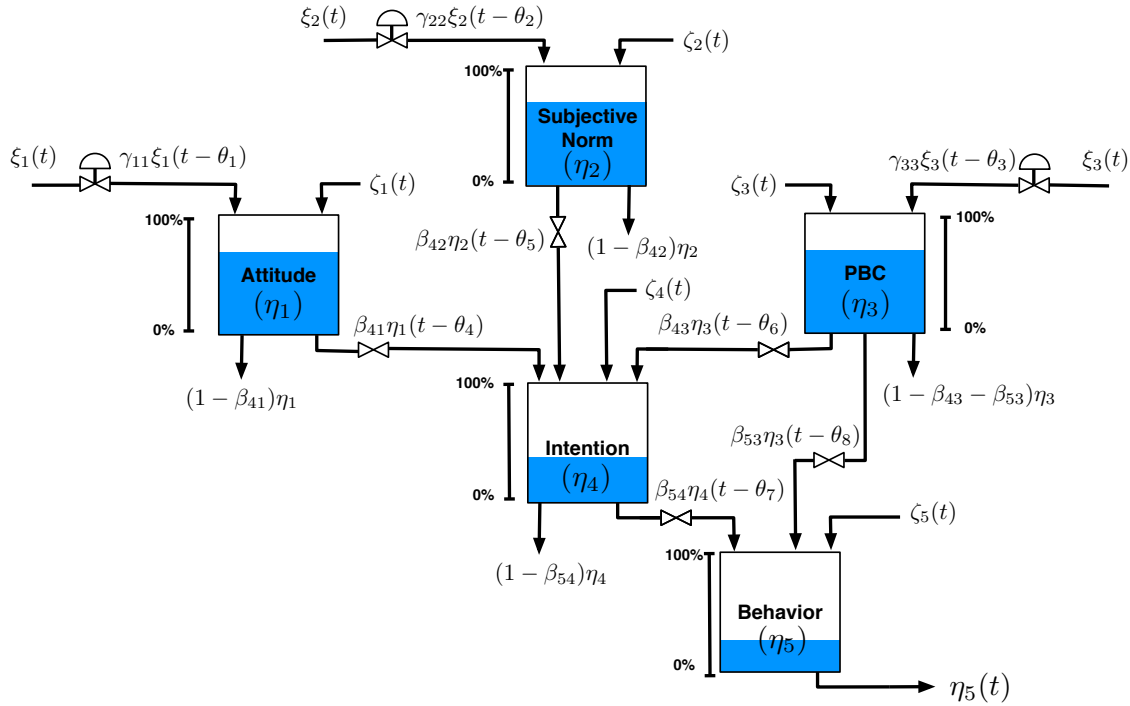


Figure 2. Proposed Fluid Analogy for TPB corresponding to diagram shown in Figure 1 (Navarro-Barrientos *et al.*, 2011).

In this analogy, each of the constructs is represented as an inventory with level

η_i , which increases or decreases based on the inflows and outflows. The variables γ_{ij} and β_{ij} represent inflow resistances and outflow resistances, respectively. η_i are the exogenous inputs, ζ_i is a zero-mean stochastic signal affecting inventory i , and θ_i stands for time delays between each inflow or outflow and their respective inventory.

For each inventory, a material balance based on the conservation of total mass can be applied:

$$\text{Rate of Accumulation} = \text{Inflow Rate} - \text{Outflow Rate} \quad (1.12)$$

When this material balance is applied to each inventory, a differential equation is generated. With five inventories, five differential equations would be generated in this TPB example, forming the set of dynamic equations that define the system:

$$\begin{aligned} \tau_1 \frac{d\eta_1}{dt} &= \gamma_{11}\varepsilon_1(t - \theta_1) - \beta_{41}\eta_1(t) - (1 - \beta_{41})\eta_1(t) + \zeta_1(t) \\ &= \gamma_{11}\varepsilon_1(t - \theta_1) - \eta_1(t) + \zeta_1(t), \\ \tau_2 \frac{d\eta_2}{dt} &= \gamma_{22}\varepsilon_2(t - \theta_2) - \beta_{42}\eta_2(t) - (1 - \beta_{42})\eta_2(t) + \zeta_2(t) \\ &= \gamma_{22}\varepsilon_2(t - \theta_2) - \eta_2(t) + \zeta_2(t), \\ \tau_3 \frac{d\eta_3}{dt} &= \gamma_{33}\varepsilon_3(t - \theta_3) - \beta_{43}\eta_3(t) - \beta_{53}\eta_3(t) - (1 - \beta_{43} - \beta_{53})\eta_3(t) + \zeta_3(t) \\ &= \gamma_{33}\varepsilon_3(t - \theta_3) - \eta_3(t) + \zeta_3(t), \\ \tau_4 \frac{d\eta_4}{dt} &= \beta_{41}\eta_1(t - \theta_4) + \beta_{42}\eta_2(t - \theta_5) + \beta_{43}\eta_3(t - \theta_6) - \beta_{54}\eta_4(t) - (1 - \beta_{54})\eta_4(t) + \zeta_4(t) \\ &= \beta_{41}\eta_1(t - \theta_4) + \beta_{42}\eta_2(t - \theta_5) + \beta_{43}\eta_3(t - \theta_6) - \eta_4(t) + \zeta_4(t), \\ \tau_5 \frac{d\eta_5}{dt} &= \beta_{54}(t - \theta_7) + \beta_{53}(t - \theta_8) - \eta_5(t) + \zeta_5(t) \end{aligned} \quad (1.13)$$

Where τ_i represents a time constant for inventory i . All the differential equations in Equation 1.13 represent a transient, dynamic system. When the derivative terms

are set to 0 (stationary, or steady-state), the equations correspond to those obtained by the SEM model (Navarro-Barrientos *et al.*, 2011).

As mentioned previously, Equations 1.13 were derived on the basis that this behavioral system is linear and all inventory equations were considered first order equations. The problem of fluid analogy complicates with the presence of higher order equations and nonlinearities, but the example was still helpful to showcase how fluid analogy can be used to create a set of differential equations from only a qualitative stationary structure path diagram originated from a behavioral theory. With these equations and measured input-output data from experiments, semi-physical modeling can be performed in order to estimate the many parameters τ_i , β_{ij} , γ_{ij} , and θ_i , thus obtaining a quantitative dynamic model.

This example shows how to use fluid analogy in order to obtain a set of differential transient equations based on a behavioral theory, but the inverse path is also a possibility. That is, if a mathematical model is obtained for a system (e.g., obtained through black-box modeling), the equations can be described in terms of a set of inventory-flows (fluid analogy), which can then be reinterpreted as a structural path diagram. In that way, the fluid analogy is not only useful to obtain mathematical equations from a behavioral theory, but it can also be used to obtain insights about behavioral theories based on experimental input-output data.

1.7 Model Validation

Simply estimating the dynamic models is not sufficient to identify a system. It is also of vital importance to validate the model, which is, to determine if the obtained model is "good enough" to represent, predict, or simulate the studied system.

According to Ljung (1999), some aspects to be considered when validating a model are whether it agrees (to a reasonable point) with the measured data, and whether it describes the true system (if not perfectly accurate - which might be close to impossible - at least to a good enough degree for the identification purposes).

One of the most common ways of validating, or testing, a model is to simulate it with the experimental data set. In this way, the same collected input data that was used for identification is used as an input for the model, which is simulated and generates some output data (since a model describes the dynamic relation between input and output). If the model happens to be an accurate description of the true system, this generated output should match, or at least be very similar to, the experimental output; otherwise, a "poor" model would generate vastly different output signals for the same inputs.

Mathematically, this proximity between generated output and simulated output can be represented by a scalar called goodness-of-fit, according to:

$$Goodness-of-Fit [\%] = 100 \left(1 - \frac{\|y(t) - \tilde{y}(t)\|_2}{\|y(t) - \bar{y}\|_2} \right) \quad (1.14)$$

In Equation 1.14, the vector of measured output data is $y(t)$, it's average is \bar{y} , and $\tilde{y}(t)$ is the vector of simulated output (generated by the model). The $\| \cdot \|_2$ notation indicates the 2-norm - the square root of the sum of the squared vector elements. Goodness-of-fit can range from minus infinity (an infinitely bad model, incapable of describing the system) to 100% (the model-generated output is exactly the same as the experimental output data, that is, the model is a perfect descriptor of the dynamics). A goodness-of-fit of 0 means that the output vector generated by the model is the same as the averaged measurements, \bar{y} .

A better way of validating a model is with cross-validation, which gives a better

determination of the predictive ability of the model. If the data collection experiment generates a sufficiently big data set, that set can be divided into estimation data and validation data. Estimation data is used in the system identification procedure (e.g. parametric estimation) to obtain a dynamic model. That model is then compared not against the same data set, but instead with the validation data set. Instead of running the model with the experimental input to generate a simulated output, and compare this with the experimental output, the model is simulated with the validation data set input, and the simulated output is compared with the validation data set output (using some criteria such as the goodness-of-fit). In this way, one set of data is used solely to generate a model, and another set of data uses only to validate it. This method of model validation is usually preferred upon, since it tests the model's capacity of predicting the output. The problem with this method lies in the fact that generating a large enough data set to be split in two (estimation and validation) can be difficult. The model estimation is a step that benefits from a large data set (ideally, infinite data points); if that data set is split into estimation and validation, the model quality may be compromised.

Sometimes, simply analysing the identified model responses grants insight upon the model validity. Simple model responses, such as the step response (as in, the output signals generated by a step change in one or more inputs) may be analysed and yield information about the system. This form of validating can be useful if prior theoretical knowledge of how the system should behave is at hand, which may allow for the modeled responses to be put into contrast against the intended output behavior. A similar analysis can be made to the identified model's frequency response, which might grant information about the frequency content of the modeled system, allowing for comparisons with any prior knowledge about the true system.

Another common method of model validation is residual analysis. The difference between simulated output and experimental output generate an error vector. Ideally, if the model is a good representation of the true system, this error should only represent measurement noises, instead of modeling errors such as bias. For this reason, an analysis of the error sequence might grant or remove validity to a model; a good model will contain a sequence of errors that is a white-noise sequence (that is, a sequence of independent random variables), and that should have no cross-correlation with any input sequences (Ljung, 1999).

There are many other aspects to analyse when doing model validation, such as the mathematical/physical feasibility of the identified parameters (as in, even if an identified model shows good fit and adequate responses, some parameters values or ranges might make no physical sense). There is no exclusive way of determining if an identified model really corresponds to the true system.

Chapter 2

BLACK-BOX SYSTEM IDENTIFICATION IN OBSERVATIONAL BEHAVIORAL STUDY

2.1 Overview

In this first case study, black-box ARX modeling was used to obtain model structures relating behavioral constructs (negative affect and self-efficacy) with physical activity (the desired behavior). This analyzed set of data came from a study called Project MOBILE (Measuring our Own Behavior in Living Environments), which had the purpose of investigating the effects of environmental and intrapersonal factors into health behavioral decisions (Dunton *et al.*, 2015)).

The data used for system identification purposes was obtained for over 90 participants by measuring, for each participant, the amount of moderate-to-vigorous physical activity (MVPA), as well as measuring the investigated self-reported behavioral constructs, among other assessments, throughout the course of four days, after scheduled prompts from a mobile phone app. The gathered data was averaged among the participants divided by different cohorts - segregating data by age, gender, and BMI category - and using different combinations of estimation-validation sets. Classical system identifications techniques were performed to obtain the dynamic structures.

As will be developed in this chapter, the results implies that the behavioral systems regarding the studied variables are actually under the influence of self-regulatory processes, akin to controllers in traditional engineering systems.

The theoretical dynamic relations between the studied variables – negative-affect and self-efficacy; and then self-efficacy and behavior – come from the well-established Social Cognitive Theory (SCT) (Bandura, 1986). According to Locke and Latham (1990), the behavioral dynamics of this systems can be seen in Figure 3:

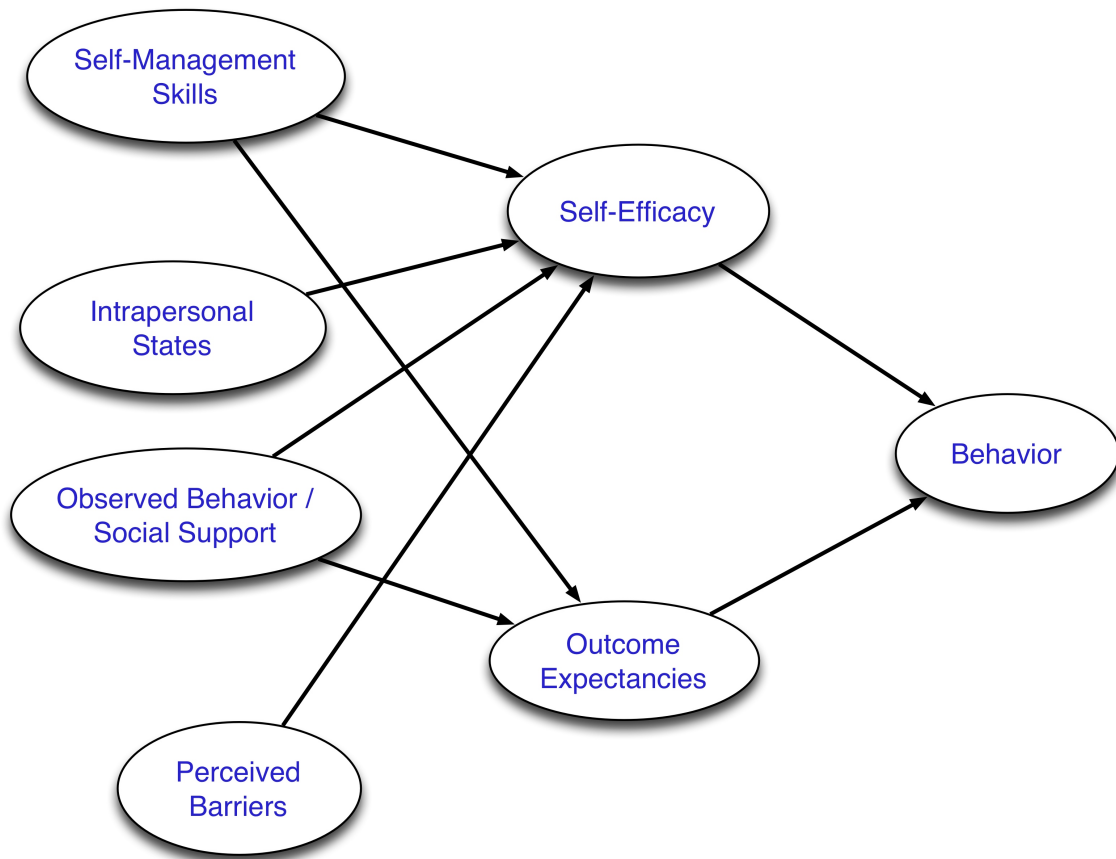


Figure 3. Open-loop Behavioral Model from Social Cognitive Theory

With black-box modeling, the exact structure of the system is not needed in order to obtain dynamic models between variables of choice. So for the purposes of this study, only a sub-set of this dynamic system was chosen: the relation between negative affect (one of the Intrapersonal States), Self-Efficacy, and Behavior (in this case, the studied behavior is MVPA). The simplified structure can be seen in Figure 4:

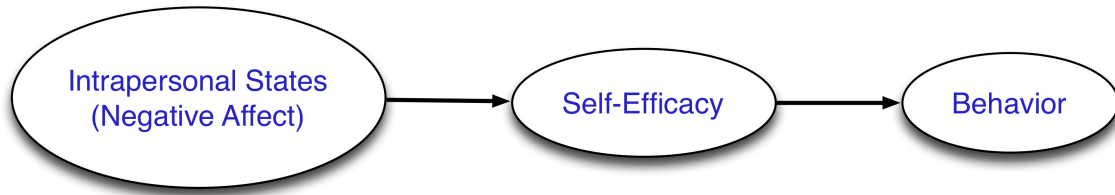


Figure 4. Simplified Open-loop Behavioral Model

So, in this study, two identification problems were carried out; one for each of the constructs relationship seen in Figure 4 above.

2.2 Data Collection Overview

Performing black-box system identification requires a good amount of informative, time-varying data in the form of time series, continuous or discrete. With recent technological advances, it is easy to obtain such time-intensive data for physical activity-related measurements. Constant positioning can be easily tracked with Global Positioning System (GPS); heart rate can be measured directly during a physical activity session; numbers of daily walked steps can be monitored with smartphones or fitness trackers. These are but a small number of examples of how mobile sensors allows the gathering of time series useful for health behavioral studies, at least with regards to physiological variables.

Psychological variables, such as affective feeling states and social-cognitive beliefs, can also be measured in a similar fashion. Ecological Momentary Assessment (EMA) or Experience Sampling Methods (ESM) (Kaplan and Stone, 2013; Shiffman *et al.*, 2008) is a data-collection technique used to obtain real-time information about participants. By this method, at the moment and place the behavior is happening, the research participants input self-reports about emotional states, attitudes, beliefs, and perceptions

with a smartphone (or other mobile device). When these self-reports are repeated throughout the length of an experiment, this in-context information assessment is able to be treated as a time series, showing how these behavioral constructs vary over time prior to, during, and after the behavior (Dunton *et al.*, 2015)). Thus, EMA and ESM allows for visualization of time-varying intra-individual assessment (Dunton and Atienza, 2009; Dunton *et al.*, 2009).

The self-reported methods provided by EMA and ESM allow for the time-intensive measurement of many behavioral variables such as physical and social contexts (Shiffman *et al.*, 2002), environmental perceptions (Dunton *et al.*, 2012), affective and physical feeling states (Dunton *et al.*, 2014; Shiffman *et al.*, 2007), and social-cognitive beliefs – like self-efficacy (Hekler *et al.*, 2012).

EMA and ESM methods are being more used in research involving health behavior, since the time-series analysis provided by these techniques can provide insights into the determinant causes of a behavior, as well as reducing recall error and biases (since reports are made at the context the behavior is happening) (Kaplan and Stone, 2013). Because mobile phones are common and easy to use, EMA and ESM data can be quickly gathered from large numbers of people and the information can be easily transferred to remote servers for data analysis (Patrick *et al.*, 2008; Riley *et al.*, 2011). For these reasons, EMA and ESM have been used to investigate health-related behavior in a number of recent studies. This includes physical activity (Dunton *et al.*, 2011a,b), eating (Carels *et al.*, 2004), smoking and substance use (Piasecki *et al.*, 2014; Freisthler *et al.*, 2015; Swendsen *et al.*, 2014), and risky sexual behaviors (Roth *et al.*, 2014), among others.

2.3 Participants and Recruitment

Three EMA data collection waves were performed, each separated by six months (although this work only focused on the second data wave). No data was gathered in the periods of late July to August and January (since extreme temperatures and weathers can significantly alter physical activity behaviors). Each wave consisted of data being assessed in 4 consecutive days. System identification analysis for this study were made using data from the second wave only, for being more complete in terms of data points. Also, data points from the first collection are more prone to report error due to potential reactivity, social desirability, and lack of familiarity associated with completing the EMA questionnaire (Dunton *et al.*, 2015)).

A total of 95 participant data was used for the dynamic analysis of the relation between negative affect and self-efficacy, and data from 93 participants used to study the relation between self-efficacy and physical activity (MVPA in the following 60 minutes). The actual number of participants involved in the second data collection wave (the one used in this analysis) was 97 (out of a total of 116 participants enrolled in the study), but some did not provide all the necessary EMA or accelerometer data. Participant ages ranged between 28 and 74 years, with an average of 40.3 years. Most participants were female (72%) and overweight or obese (63%).

Participants chosen for the data collection included healthy adults living in Southern California that met the following criteria: age of 25 years or older; fluent English speaker and reader; able to answer electronic EMA surveys while at work; and willing to wear an accelerometer. Were excluded those participants with an annual household income greater than \$210,000, those who regularly performed more than 150 minutes per week of exercise or physical activity, and/or those with physical limitation that

makes them unable to perform exercises. These exclusions happened because the main goal of the larger study was to evaluate physical activity behaviors for participants at elevated risk for obesity, which means low active and low-to-moderate income individuals.

Physical activity levels (MVPA) were measured by a waist-worn accelerometer used by the participants during waking hours across the four days of each wave. Behavioral EMA data were collected by a mobile phone through the MyExperience software (Froehlich *et al.*, 2007). Eight EMA surveys were prompted each day, at random times between 6:30am and 10:00pm, to gather information about negative affect, self-efficacy, and other variables. Each of these prompts required about three minutes to complete, and the prompt were to be ignored in case the participant could not answer at the time (for instance, if he or she were bathing) – in that case, the phone asked for another survey after five-minutes, up to three reminders.

For the affect assessment, EMA used the bi-dimensional circumplex model consisting of valence (varying between pleasure and displeasure) and arousal (varying between activation to deactivation), where negative affect represents the combination of activated displeasure (e.g., nervous, anxious or stressed) and deactivated displeasure (e.g., sad, depressed or frustrated) (Posner *et al.*, 2005). EMA prompts response options for each of these affective states were “Not at all”, “A little”, “Moderately”, “Quite a bit”, and “Extremely”.

The other behavioral variable used in dynamic modeling was self-efficacy, which momentary levels were measured with the EMA through two questions: “Can you do at least 10 minutes of physical activity sometime within the next few hours even if you get busy?”, and “Can you do at least 10 minutes of physical activity sometime within the next few hours even if you start to feel tired?”. These questions, based on

pervious EMA studies, were delivered through a 5-point response scale (with 1 being “I know I cannot” and 5 being “I know I can”) (Freisthler *et al.*, 2015; Swendsen *et al.*, 2014; Roth *et al.*, 2014).

Only 60% of the total EMA prompts – chosen randomly - included affect assessments (including both negative affects and positive affects, which were measured but not used in the system identification analysis) to avoid potential participant burden, while only 40% of the EMA assessments included self-efficacy questions for the same reasons. So, the chances of a participant receiving both negative affect and self-efficacy assessments (both used in the dynamic modeling) in the same prompt was 24% (60% x 40%).

On the 5-point response scale used to measure negative affect and self-efficacy, the average negative affect rating was 1.4 (with 0.4 standard deviation), and for self-efficacy a 3.0 (with 0.8 standard deviation) rating was the average. Concerning physical activity, the average time participants spent doing moderate-to-vigorous physical activity was 1 minute (with 0.7 standard deviation) after each EMA prompt.

2.4 Data Analysis and Pre-Treatment

Some analysis and treatment to the collected EMA and accelerometer data were performed prior to the system identification processes.

Participant data, originated from Excel-sheets, contained, for each participant, 8 prompt answers for each of the four days of the data wave (for a total of 32 data points per participant). However, not all participants answered the same number of prompts at the same times, due to the nature of the experiment – since not every EMA prompt asked for a negative affect or a self-efficacy measurement.

The data collection happened in a limited time interval each day – ranging from around 6.30am to 10pm – and thus there was a long period of no data collection after the last point in a day (around 10pm) and the first point of the next day (around 6.30am). For that reason, instead of making one time series for each participant containing all the 32 data points, each day was considered its own experiment, so four different time series were generated for each participant. These were designated by the numbers 1 (Saturday), 2 (Sunday), 3 (Monday), and 4 (Tuesday) – each being one of the days in which data collection happened.

System identification techniques can be used for an idiographic (focused on each subject individually) study, but in the case of this research, because of the lack of some data points, it was decided to generate time series by averaging the participant’s data. To visualize and compare the interplays between negative affect, self-efficacy, and MVPA happening amongst different participant groups, participant data were also separated into different cohorts. So, for each cohort, four time series (one for each day) were generated by averaging all the daily data for all participants in that cohort.

The cohorts have been divided in a way that, in theory, different output responses would be obtained, meaning that the interconnections between variables would be different. In other words, the identified model structure, shape of response, and/or parameters would be different for each cohort. With that in mind, the analyzed cohort divisions were aggregation by age (one cohort for participants with age less than the median, and another for participants with age higher than the median); by gender (one cohort for male participants, and another for female participants); and lastly, an aggregation by BMI category (one cohort for participants considered Underweight/Normal, and another cohort for Overweight/Obese participants). The median age for all participants was 39 years.

So, summarizing the cohort division, the time series created in the data pre-treatment phase were:

1. Four time series (one for each day) averaging all participants data (95 participants);
2. Four time series (one for each day) averaging participants with age less than median data (46 participants);
3. Four time series (one for each day) averaging participants with age more than median data (45 participants);
4. Four time series (one for each day) averaging male participants data (26 participants);
5. Four time series (one for each day) averaging female participants data (67 participants);
6. Four time series (one for each day) averaging underweight/normal participants data (34 participants);
7. Four time series (one for each day) averaging overweight/obese participants data (60 participants).

The total is 28 time series. All this analysis was made only for one of the input-output relations. Considering there was two identification problems to be studied (negative affect and self-efficacy; and self-efficacy and MVPA), the actual total number of time series generated was 56.

Each of these time series was transformed into an `iddata` object, necessary for being used in MATLAB's System Identification Toolbox. These `iddata` objects contain the input and output time series – in the first identification problem, these were negative affect and self-efficacy, respectively; in the second problem, self-efficacy and MVPA in the following 60 minutes after the EMA prompt, respectively.

A plot showing one of these time series for this study is shown below. Because of the large number of different time series (depending on studied cohort and experiment day), it is unfeasible showing all the possible plots here; Figure 5 shows a representative time series - in this case, for the averaging of all participants in Day 1 (Saturday).

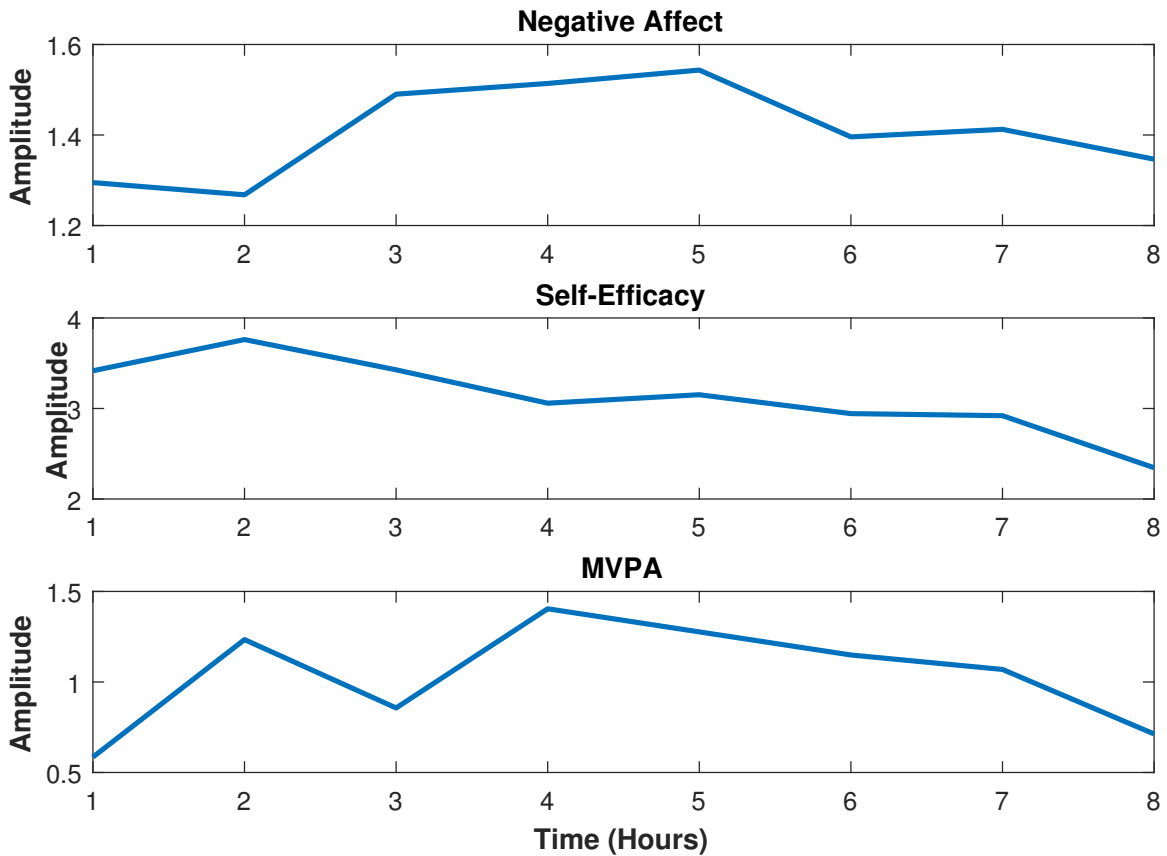


Figure 5. Representative Time Series Used Prior to Identification - All Participants, Day 1

Although Figure 5 does not explicit the dynamic relations between these constructs, it is useful to allow some patterns to be visualized. The Figure indicates that the averaged participant at this day presents two peaks of moderate-to-physical activity throughout the day (one in the morning and one in the afternoon). Self-efficacy begins at a higher level in the morning, but then decreases at the end of the day, while

negative affect begins in a low level, increases in the middle of the day, and then returns to a value closer to the initial level. Data for other cohorts and/or experiment days, although being different in details, also show this pattern of decreasing self-efficacy, peaks in MVPA, and rise-and-fall of negative affect.

2.5 ARX Modeling

With all the time series in hand, proper system identification was used to obtain model structures. This was done using MATLAB's System Identification Toolbox through the `ident` command, which opens the system identification app. A representative image of the toolbox being used for identification purposes can be seen in Figure 6.

For this study, the chosen model structure to attempt data fitting were ARX (AutoRegressive with eXternal inputs) models. This is a very common prediction error model structure with many advantages from a theoretical point of view, such as consistency. It is always straightforward to perform identification through this model structure. Ljung (1999) recommends, for most identification problems, to initially try ARX modeling as a standard approach to parameter estimation, and only if the obtained models are not sufficiently good, trying other approaches.

ARX models represent the following structure:

$$y(t) + a_1 y(t-1) + \dots + a_{n_a} y(t-n_a) = b_1 u(t-n_k) + \dots + b_{n_b} u(t-n_k-n_b+1) + e(t) \quad (2.1)$$

Equation 2.1 is for a single-input, single-output system; the structure is expanded for multiple inputs and/or outputs, but that is not the case in this study. Here,

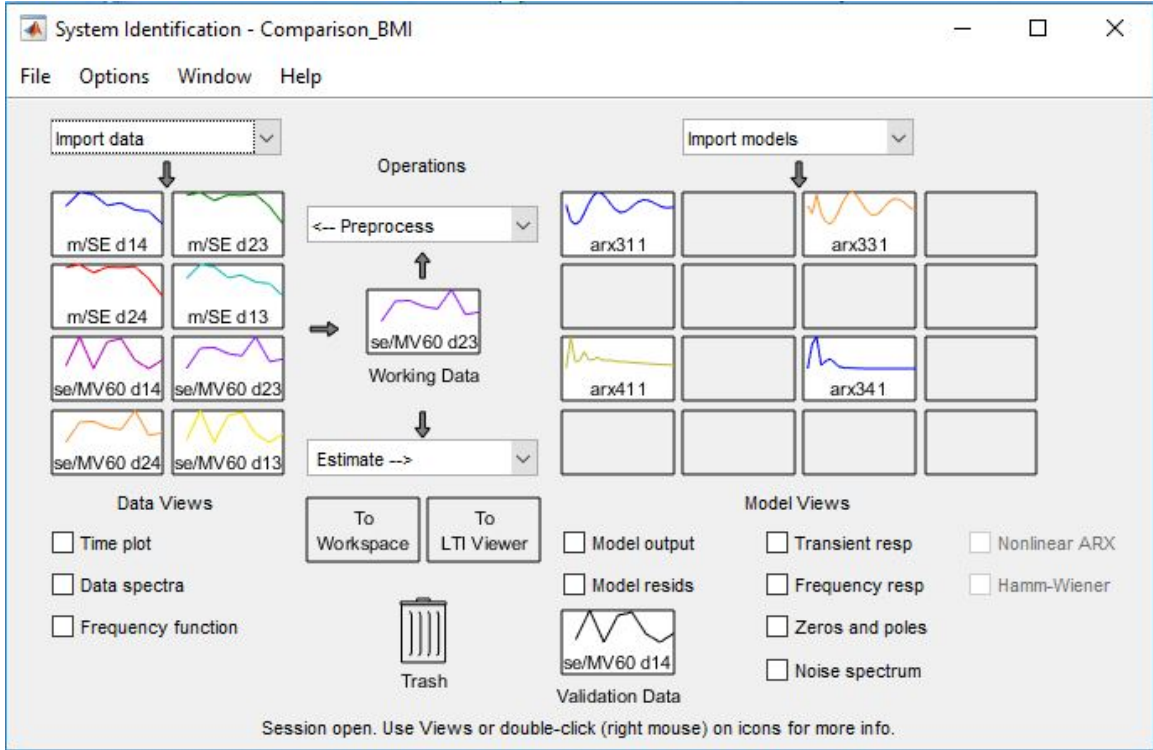


Figure 6. Representative System Identification Toolbox App Window

$y(t)$, $u(t)$ and $e(t)$ represent the outputs, inputs, and a white-noise term, respectively; $[a_1, \dots, a_{n_a}, b_1, \dots, b_{n_b}]$ are the parameters to be estimated, and n_a, n_b, n_k represent the orders of the model. The number of inputs and outputs is determined by the studied problem and included in the `iddata` objects that contains the measured time series; the model's order, on the other hand, is specified by the user prior to starting the identification computations. For this reason, ARX models are always named in conjunction to stating the model's order (ARX $[n_a \ n_b \ n_k]$) – for example, ARX $[4 \ 4 \ 1]$ is a model with structure following Equation 2.1 with $n_a = 4, n_b = 4, n_k = 1$, and thus 8 parameters to estimate.

Since the user specifies the structure order to try to find the best fits, this method is inherently interactive. If a certain order does not provide a good result (based on the model validation criteria), another structure order can be chosen and the

computations are repeated. The choice of structure order depends naturally on the problem. Usually, ARX requires relatively high orders to generate a good model if there is significant noise present (Ljung, 1999); on the other hand, there is the problem of over parametrization – that is, deciding for a model order higher than what it is needed to capture a good model. Usually, parsimonious models (that is, models with the lowest amount of parameters necessary) are sought for, because they are easier to interpret physically and to work on computationally. A good recommendation made by (Ljung, 1999) for some cases is to start with an ARX [4 4 1], which, in most situations, provide a good balance between model flexibility and over parametrization, and then increase or decrease the order as necessary (Dunton *et al.*, 2015)).

For experiments with enough data points are available so that estimation and validation data can be used, the System Identification Toolbox app (used for the modeling in this study), in MATLAB, offers an **Order Selection** feature for ARX estimation. With this feature, the user defines a model order range for each parameter (usually 1-10 for all parameters – this is input as $n_a = [1 : 10]$, $n_b = [1 : 10]$, $n_k = [1 : 10]$), and then the software will exhaustively obtain all models in the range and provide their goodness-of-fit for comparison (other model validation criteria, such as step response, are not as readily available, but the user can reproduce any model structure for individual inspection).

Because of the limited amount of data points, however, it was impossible to identify ARX model orders higher than ARX [4 4 1] due to software limitations based on the amount of data points. For this reason, the **Order Selection** features was performed by ranging $n_a = [1 : 4]$, $n_b = [1 : 4]$. For the sake of model simplicity, no time delay was considered, so n_k was left at a constant value of 1.

For this study, that was the procedure used to obtain dynamic models. For each

of the 56 `iddata` objects generated in the data processing step, a good ARX model was searched using the `Order Selection` feature, as well as individual investigation of generated models in most cases.

In the System Identification Toolbox app, when a polynomial model (such as ARX) structure is decided upon for identification, the user has an option to decide the focus of identification procedure: prediction, simulation, stability, or a user-defined filter. This identification option is related to how the loss function is minimized (Equations 1.4 and 1.5) (MathWorks, 2016a). Usually the prediction focus is used as a system obtained this way provides a better indicator of the predictive capacity of the model; for this study, however, prediction focus generated unstable models (possibly due to the small amount of data points in each time series). For this reason, stability focus was opted for, which enforces an additional constraint - that the identified model must be stable - in the computing process.

2.6 Model Validation

After an ARX model was generated, it needed to be validated. Model validation was done in the following ways. Firstly, scalar goodness of fit (as described earlier, defined by Equation 1.14) was used to compare models, but not great emphasis on this validation method was given. Goodness of fit might not be a perfect indicator of model quality if the data collection was not designed with system identification in mind, following the steps of good experiment design. Also, the small amount of data points for each experiment day hinders the model quality.

The focus given was, instead, to the step response. The models that best describe the dynamical system were based on the works of Dunton *et al.* (2015), that is,

following similar shape of response; underdamped with negative gain for the negative affect to self-efficacy problem, and overdamped with positive gain for the self-efficacy to MVPA60 problem.

Models with step response that deviated from these responses were discarded, as well as models with unreasonable or impossible responses (like those with extremely high settling time which does not make sense in a real world behavioral scenario).

By splitting all the time series into each of the four days the experiment took, it was decided to use the data for half the days for model estimation, and the other half for model validation. With the four experiment days, there are six possible pairs of estimation data; these are [1,2], [1,3], [1,4], [2,3], [2,4], and [3,4], with the opposite pair used for validation. However, only four of these pairs combine a weekday and a weekend-day ([1,3], [1,4], [2,3], [2,4]). Each model was generated and analyzed for each of these four pair combinations, to avoid the possibility of behavioral differences occurring from a weekend and a week-day interfering in the models.

Another way of validating model that was evaluated was considering all days for estimation and all days for validation. In this way, all the generated `iddata` objects contained the four days (as four different experiments), and participant data was split in two; one half for estimation and the other for validation. However, for most cases this resulted in worse models (either from a goodness-of-fit or from a system's response perspective), with the exception of the `iddata` created by all participants (no cohorts). This might be because, when splitting participants in cohorts, each cohort has naturally fewer number of participants. Upon further splitting into half participants for estimation and half for validation, the number of participants decrease too much for each `iddata` object and that compromises the quality of the model.

2.7 Results and Discussion

Important information about all the estimated models is summarized in Tables 2 and 3, which details the identified ARX order, which days were used for estimation and which for validation, and the models' goodness of fit %, for each of the cohorts. Table 2 contains information about the first identification problem (negative affect as input, self-efficacy as output), while Table 3, about the second (self-efficacy as input, MVPA as output). Estimated parameters for the identified ARX models are presented in Appendix A.

Table 2. ARX Structure, Estimation-Validation Sets, and Goodness-of-Fit for all Cohorts for First Identification Problem (NA as Input, SE as Output)

Cohort	ARX Structure	Days Used for Estimation	Days Used for Validation	Goodness-of-Fit
All Participants	ARX [2 5 1]	1, 2, 3, and 4*	1, 2, 3, and 4*	49.03% (day 1), 27.99% (day 2), 72.43% (day 3), 51.87% (day 4)
Age				
Age < Median	ARX [4 2 1]	2 and 3	1 and 4	54.01% (day 1), 13.12% (day 4)
Age > Median	ARX [4 3 1]	1 and 4	2 and 3	30.06% (day 2), 30.46% (day 3)
Gender				
Female	ARX [4 1 1]	2 and 3	1 and 4	60.88% (day 1), 48.11% (day 4)
Male	ARX [3 3 1]	1 and 4	2 and 3	16.17% (day 2), 11.59% (day 3)
BMI Category				
Underweight / Normal	ARX [3 1 1]	2 and 3	1 and 4	52.64% (day 1), 39.05% (day 4)
Overweight / Obese	ARX [3 3 1]	1 and 3	2 and 4	31.71% (day 2), 18.33% (day 4)

*Half participants used for estimation, half participants used for validation.

Each of the identified models' step responses are discussed below, as well as comparatives against model obtained within a same data aggregation category (division by age, by gender, and by BMI category, respectively). Step response analysis is one of the most ubiquitous ways of analyzing a dynamical model. It shows how a permanent (considering the problem's time scale) unitary increase in one input will affect the outputs. Many classes of dynamic systems are well categorized and studied based on the system's step response (Ogunnaike and Ray, 1994).

Being discrete-time ARX models, these will all follow the model structure:

$$A(q)y(t) = B(q)u(t - n_k) + e(t) \quad (2.2)$$

Table 3. ARX Structure, Estimation-Validation Sets, and Goodness-of-Fit for all Cohorts for Second Identification Problem (SE as Input, MVPA as Output)

Cohort	ARX Structure	Days Used for Estimation	Days Used for Validation	Goodness-of-Fit
All Participants	ARX [3 3 1]	1 and 3	2 and 4	62.35% (day 2), 27.99% (day 4),
Age				
Age < Median	ARX [3 1 1]	1 and 3	2 and 4	61.68% (day 2), 12.18% (day 4)
Age > Median	ARX [2 2 1]	1 and 3	2 and 4	26.58% (day 1), 30.40% (day 3)
Gender				
Female	ARX [4 2 1]	2 and 4	1 and 3	33.98% (day 1), 37.79% (day 4)
Male	ARX [4 3 1]	2 and 4	1 and 3	24.24% (day 1), 32.51% (day 3)
BMI Category				
Underweight / Normal	ARX [4 1 1]	2 and 3	1 and 4	50.86% (day 1), 63.94% (day 4)
Overweight / Obese	ARX [3 4 1]	2 and 4	1 and 3	67.03% (day 2), 41.89% (day 4)

As defined by Equation 1.9, with the polynomials $C(q) = D(q) = F(q) = 1$ (defining characteristic of ARX model).

2.7.1 All Participants - General Considerations

The two Figures below show the system – identified using averaged data from all participants – step responses; Figure 7 show how a unit increase in negative affect will change self-efficacy; while Figure 8 demonstrates the effect that a unit increase in self-efficacy will have on the MVPA.

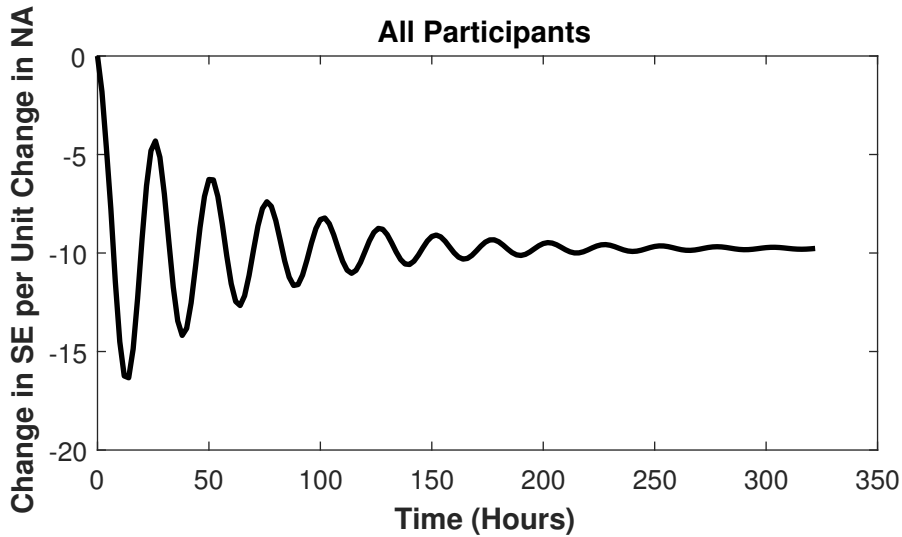


Figure 7. Step Response from NA to SE for All Participants

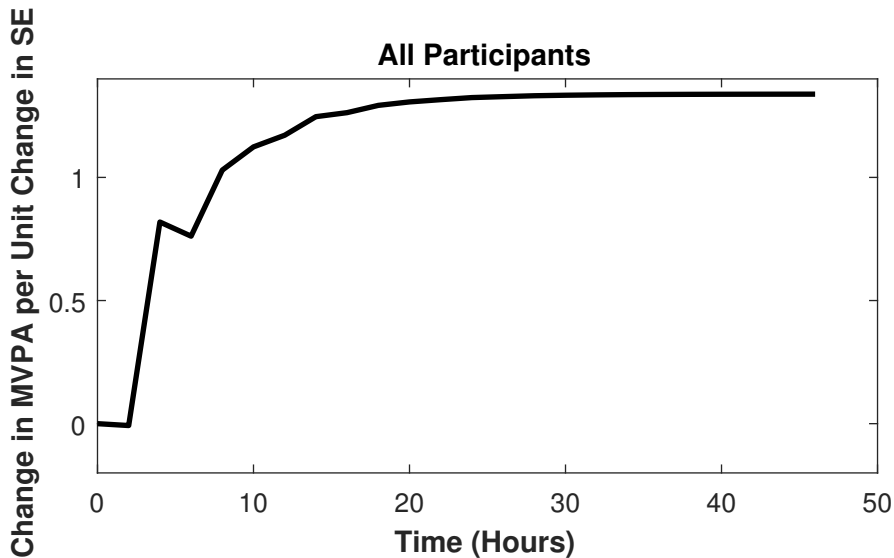


Figure 8. Step Response from SE to MVPA for All Participants

Figure 7 shows that, upon increasing the negative affect, self-efficacy will have a drastic reduction, which then oscillates back and forth – alternatively increasing and decreasing the self-efficacy value over time – until it settles down. After reaching its settling time, the output’s final stationary value will be lower than the original value, which means that the increase of negative affect will ultimately provoke a decrease in

self-efficacy levels. This is naturally to be expected – when a participant gets increased levels of displeasure (i.e. negative affect), his or her confidence in performing physical activity goes down. This is also the same shape of response reported by Dunton *et al.* (2015).

The second identification problem – self-efficacy as the input with intended behavior (MVPA) as output – is starkly different. As seen in Figure 8, a step increase in the input causes the output to smoothly increase, settling in a stationary level that is higher than the initial amount. Once again, that is easy to grasp – the more capable a participant thinks he or she is of performing the behavior, the more that participant will actually perform the behavior after the EMA prompt. Based on these responses, the transfer function between negative affect and self-efficacy has negative gain, while the transfer function between self-efficacy and MVPA is characterized by a positive gain.

Both systems also represent an open-loop stable system, which is defined by a bounded input – bounded output. In other words, a finite change in the input will lead to a response which settles in a stationary final value (Ogunnaike and Ray, 1994).

From a control systems engineering point of view, the step responses seen in Figures 7 and 8 represent well-known dynamic system types, or at least systems with similar characteristic in terms of shape of response. The oscillatory pattern of the first identification problem (negative affect to self-efficacy) is a characteristic of an underdamped system, while the smooth consistent response seen on the second identification problem (self-efficacy to MVPA) probably characterizes an overdamped system. One of the easiest ways of mathematically understanding these concepts is by analyzing a second order system, which has the following transfer function (in continuous-time):

$$\frac{y(s)}{u(s)} = \frac{K}{\tau^2 s^2 + 2\zeta\tau s + 1} \quad (2.3)$$

Where ζ denotes the damping coefficient (Ogunnaike and Ray, 1994). If ζ is less than 1, the system has imaginary poles and its response is underdamped, oscillatory; on the other hand, if it is greater than 1, the system has real valued poles, and the response will be overdamped. K , the steady-state process gain, denotes whether an increase in the input will ultimately lead to an increase or a decrease in the output.

The presence of underdamped response in the first dynamic pairing may suggest an inefficient self-regulation, such as is the case of many underdamped physical systems (Dunton *et al.*, 2015)). In other words, the effects of altering negative affect on a participant are not consistent, at least not initially – self-efficacy levels will decrease and then increase, and then decrease again, in an oscillatory pattern, until a certain settling time is reached.

The overdamped response seen in Figure 8, on the other hand, is characteristic of a system that show well-tuned regulation – as in, MVPA levels will increase or decrease consistently, in a predictable fashion, following an associated increase or decrease in self-efficacy, respectively. This result is in accordance to previous modeling studies of these variable pairings, even those using non-dynamic modeling (Dunton *et al.*, 2015).

When analyzing goodness-of-fit (in Tables 2 and 3), it can be noticed that, comparatively to the models obtained through cohort aggregation, these two models – based on data originated from all participants – have relatively high fit percentages. One possible reason for this is that, since the input and output data are averaged over a higher number of participants, random variability in the data is reduced and the model becomes better predictive.

One problem obtained with the identified model was the presence of wide confidence

intervals, meaning that estimated parameters' variance is too high. A representative example of one of the identified model's step response (from SE to MVPA for all participants), including 95% confidence intervals, is shown below in Figure 9.

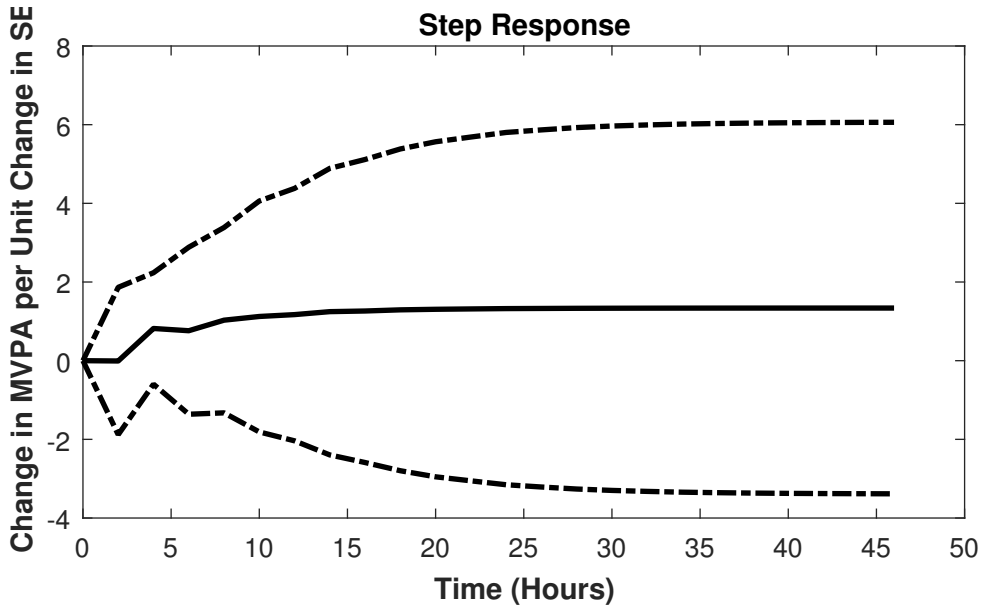


Figure 9. Step Response from SE to MVPA for All Participants Including 95% Confidence Intervals

The models obtained for cohorts other than the average of all participants (shown below) did not contain confidence intervals.

In the sections below, similar analysis will be performed for the responses of the system identified using participant data aggregated in cohorts. The overall shape of response is similar for most of the systems, though – negative affect to self-efficacy systems display negative gain, underdamped responses, while self-efficacy to MVPA function display overdamped responses with positive gains. Specific parametric values – such as the gain value, settling time, period of oscillation, or time constants - differ from one model to another, though.

2.7.2 Age Aggregation

Figures 10 and 11 show a comparison of the step-responses for both input-output pairing, comparing the responses for participants below and above the median age.

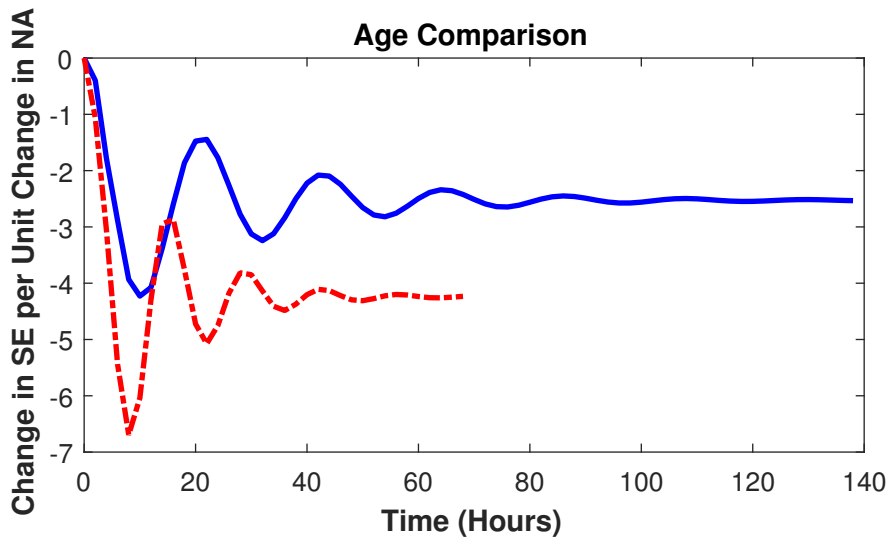


Figure 10. Step Response from NA to SE for Participants with Age Less than Median (Blue, Solid) and Age Higher than Median (Red, Dash-Dotted)

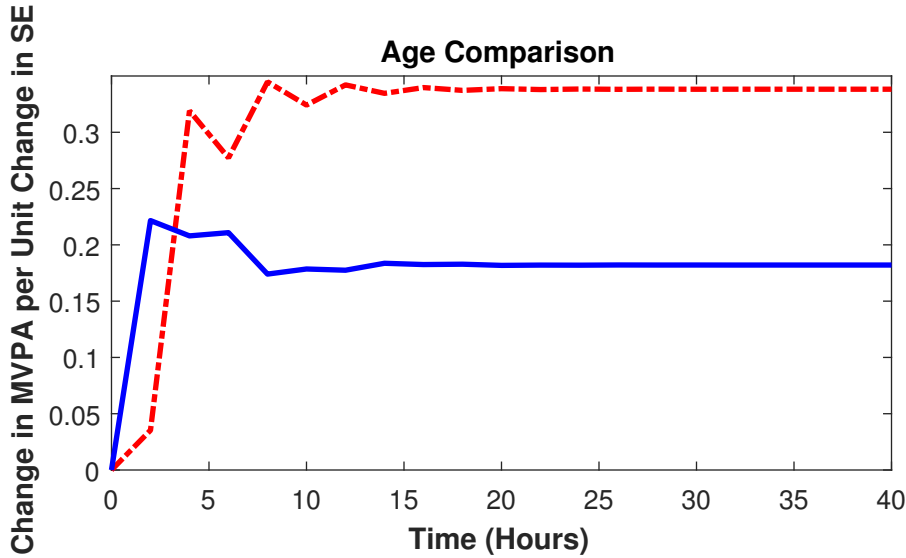


Figure 11. Step Response from SE to MVPA for Participants with Age Less than Median (Blue, Solid) and Age Higher than Median (Red, Dash-Dotted)

As noted before, the general shapes of response follow – oscillatory with negative gain for the negative affect and self-efficacy problem, and smooth consistent positive gain for the self-efficacy and MVPA problem. For the second identification problem, the systems identified with participants with age less than the median also demonstrated overshoot – that is, the response reaches levels higher than the final stationary value and then decreases to it’s steady-state level. In a dynamic systems perspective, overshoot is represented by the presence of a positive zero in the system (that is, numerator dynamics in the transfer function) (Ogunnaike and Ray, 1994).

For both identification problems, participants with higher age showed greater stationary gain – as in, after the input changes, both outputs would get greater alterations when compared to younger participants. In a behavioral sense, this would suggest that changes in behavioral constructs have a bigger impact in the participant’s dynamics for older participants, as in, they are more responsive to changes in behavioral constructs (both positive and negative).

However, it is important to note that the goodness-of-fit (seen in Tables 2 and 3) were not particularly high for this cohort aggregation. This might be because the cohort division was based on the median age (that was 39 years old), which was an arbitrary choice to split the participants. This cut point might not be a good representative division point of different behavioral dynamics.

2.7.3 Gender Aggregation

Separating participants based on gender, the step responses can be seen in Figures 12 and 13.

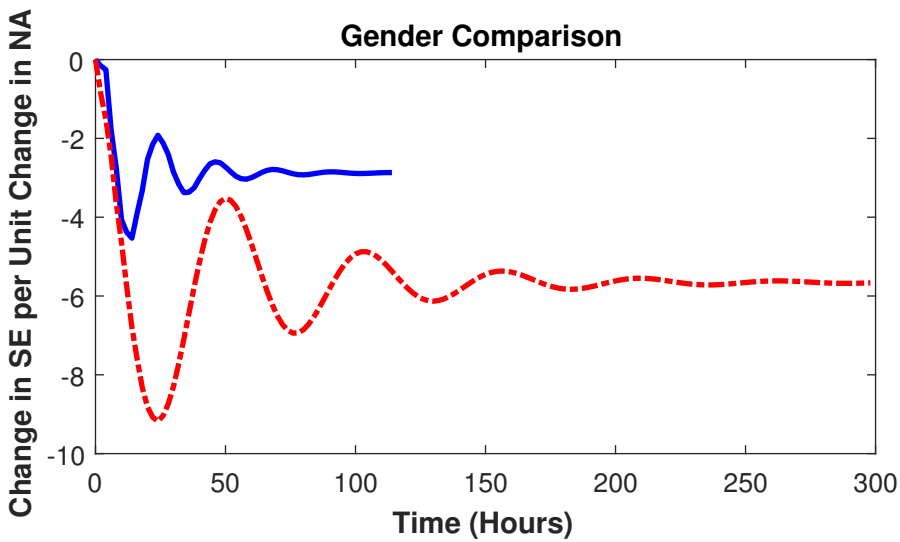


Figure 12. Step Response from NA to SE for Male (Blue, Solid) and Female (Red, Dash-Dotted) Participants

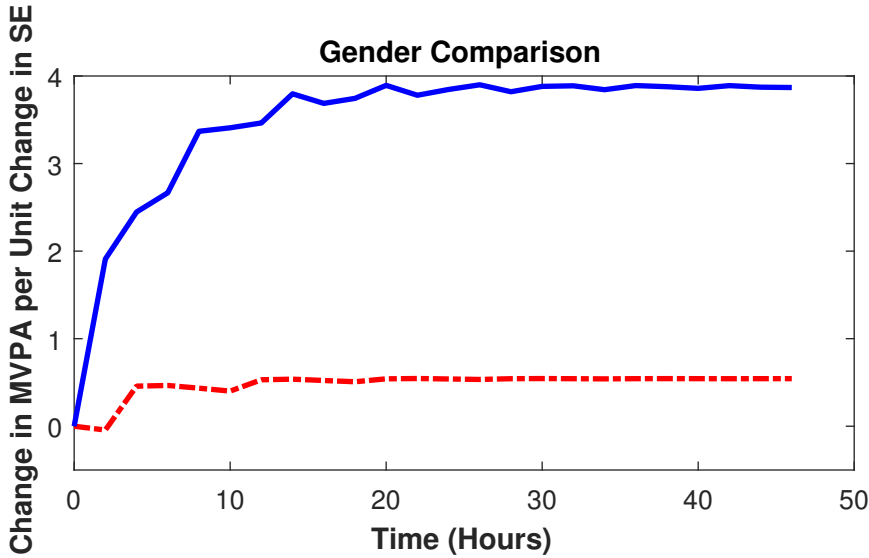


Figure 13. Step Response from SE to MVPA for Male (Blue, Solid) and Female (Red, Dash-Dotted) Participants

When comparing the responses, the Figures 12 and 13 suggest that, for the first system, female participants show higher gains and slower responses than those of the male participants. This might suggest that female participants are more influenced by negative affect changes, but that the responses take longer to reach their final value. The female cohort self-efficacy response for negative affect change (Figure 12) also shows more oscillations than the male participants', which might indicate less efficient self-regulation.

On the other hand, for the second system, the situation is inverted; male participants' stationary gain is shown to be higher. The implications of that is that, for female participants, self-efficacy does not play as strong a part in their ability to perform physical activity as vital as it does for male participants.

It is worth noticing, though, that the male participants' dynamic systems displayed poorer goodness-of-fit when compared to the female participants. The most probable reason for this is the lower number of male participants. In system identification, as

in any statistical analysis, better modeling is obtained when a larger number of data points is collected. Having way fewer participants, the quality of the male cohort modeling is naturally compromised.

2.7.4 BMI Category Aggregation

The results of the last of the cohort division, separation by BMI Category (Underweight/Normal compared against Overweight/Obese participants), can be seen in Figures 14 and 15 for the two identification problems.

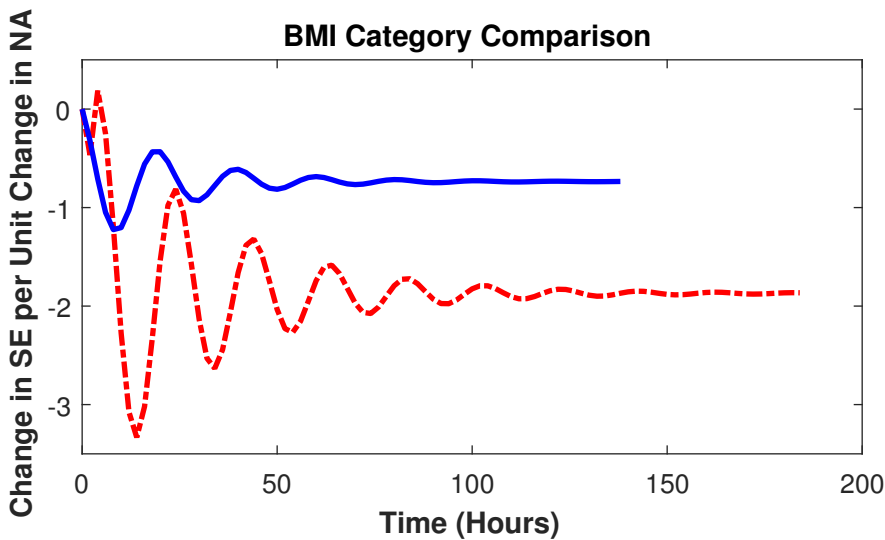


Figure 14. Step Response from NA to SE for Underweight / Normal Participants (Blue, Solid) and Overweight / Obese Participants (Red, Dash-Dotted)

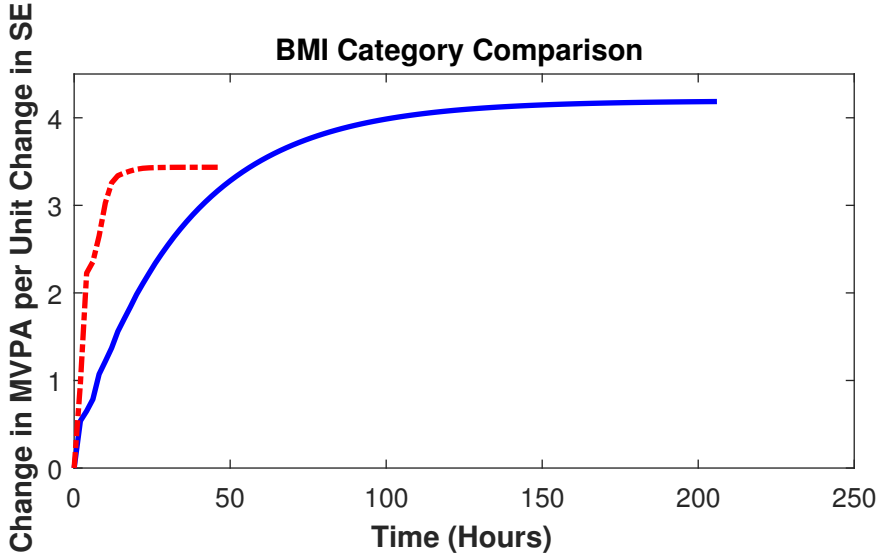


Figure 15. Step Response from NA to SE for Underweight / Normal Participants (Blue, Solid) and Overweight / Obese Participants (Red, Dash-Dotted)

For this aggregation, both cohorts showed reasonably good fit %, as can be seen in Tables 2 and 3.

These system responses suggest that, for the negative affect to self-efficacy dynamics, participants categorized as overweight or obese show higher gain, and higher settling time, than for those categorized as underweight or normal. This suggests that changes in negative affect have a bigger impact on overweight / obese participants, for these have worse self-regulation in terms of self-efficacy response.

On the other hand, for the other problem (self-efficacy to MVPA), comparatively similar gains were obtained for both cohorts. This suggests that an increase in Self-Efficacy affects participants from all BMI Categories in a similar fashion.

Best goodness-of-fit were obtained when comparing participants with this cohort division. This suggest that BMI Category might play a more influential role in determining a participant's behavioral dynamics than age or gender, and that is better to compare different participants based on this characteristic.

2.8 Control Systems Perspectives

These dynamic responses obtained from system identification techniques indicate self-regulatory behavioral processes. The ideas of behavioral self-regulation suggested by Carver and Scheier (2002, 1998) present similar system dynamics as that of an engineering system with a controller, suggesting that the open-loop diagrams showed in Figures 3 and 4 might be incomplete. A closed-loop version of Figure 4, including self-regulation, might be better represented as in Figure 16.

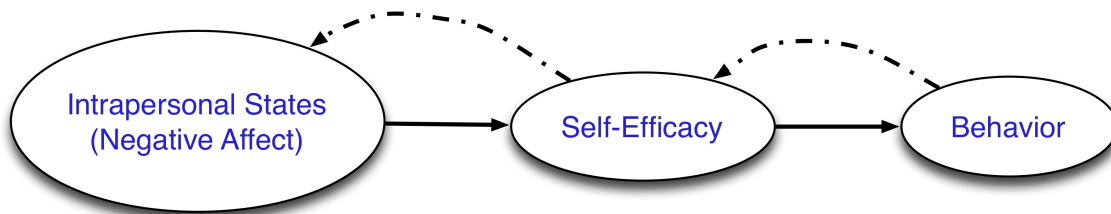


Figure 16. Closed-Loop Behavioral Dynamics

According to this theory, the dynamics between negative affect, self-efficacy, and behavior are self-regulatory. This means that, when a change in an input happens, the behavioral self-regulation processes will compare the new input to a reference value and adjust the output accordingly. When the self-regulation (e.g., control system) is poorly tuned or inefficient, the output oscillates for a short time, until the period of oscillation decreases and a stationary value is reached – such is the case when negative affect is the input and self-efficacy is the output. On the other hand, when the self-regulation process is well tuned, a change in input will provoke a consistent, smooth change in the output – such is the case when self-efficacy is the input and MVPA is the output. A diagram representing this self-regulation scheme is seen in Figure 17 (Carver and Scheier, 1998):

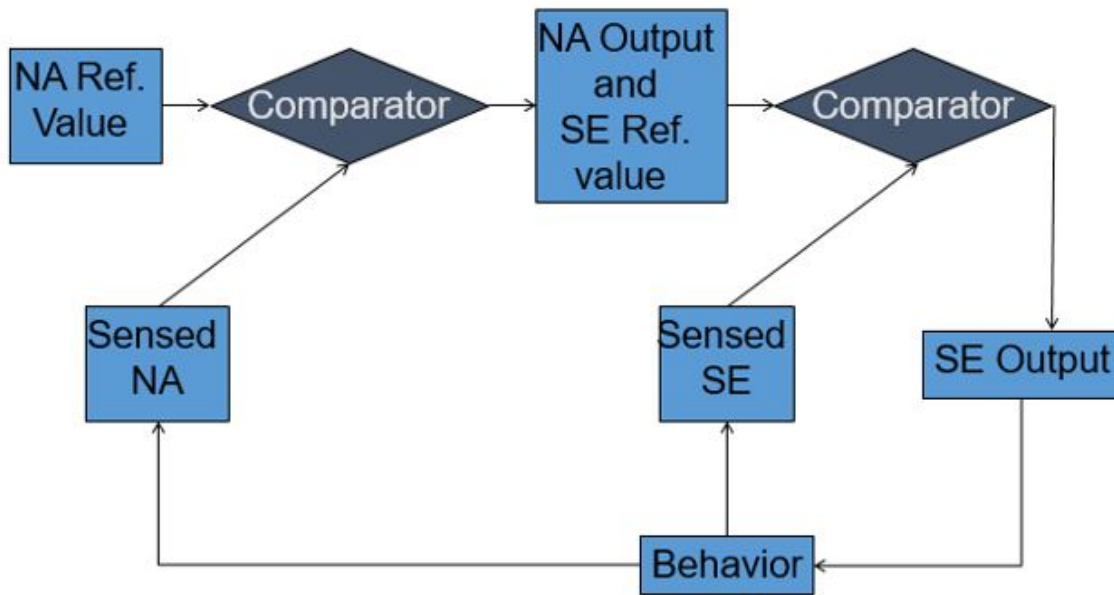


Figure 17. Behavioral Self-Regulatory Process

Where NA stands for negative affect, SE for self-efficacy, and the behavior in question is moderate-to-vigorous physical activity.

As mentioned before, this self-regulatory behavioral system can be represented in terms of a fluid analogy, making a parallel with a well-known physical dynamic system. With this analogy, the behavioral self-regulatory dynamics described here would be represented by Figure 18 (Dunton *et al.*, 2015)).

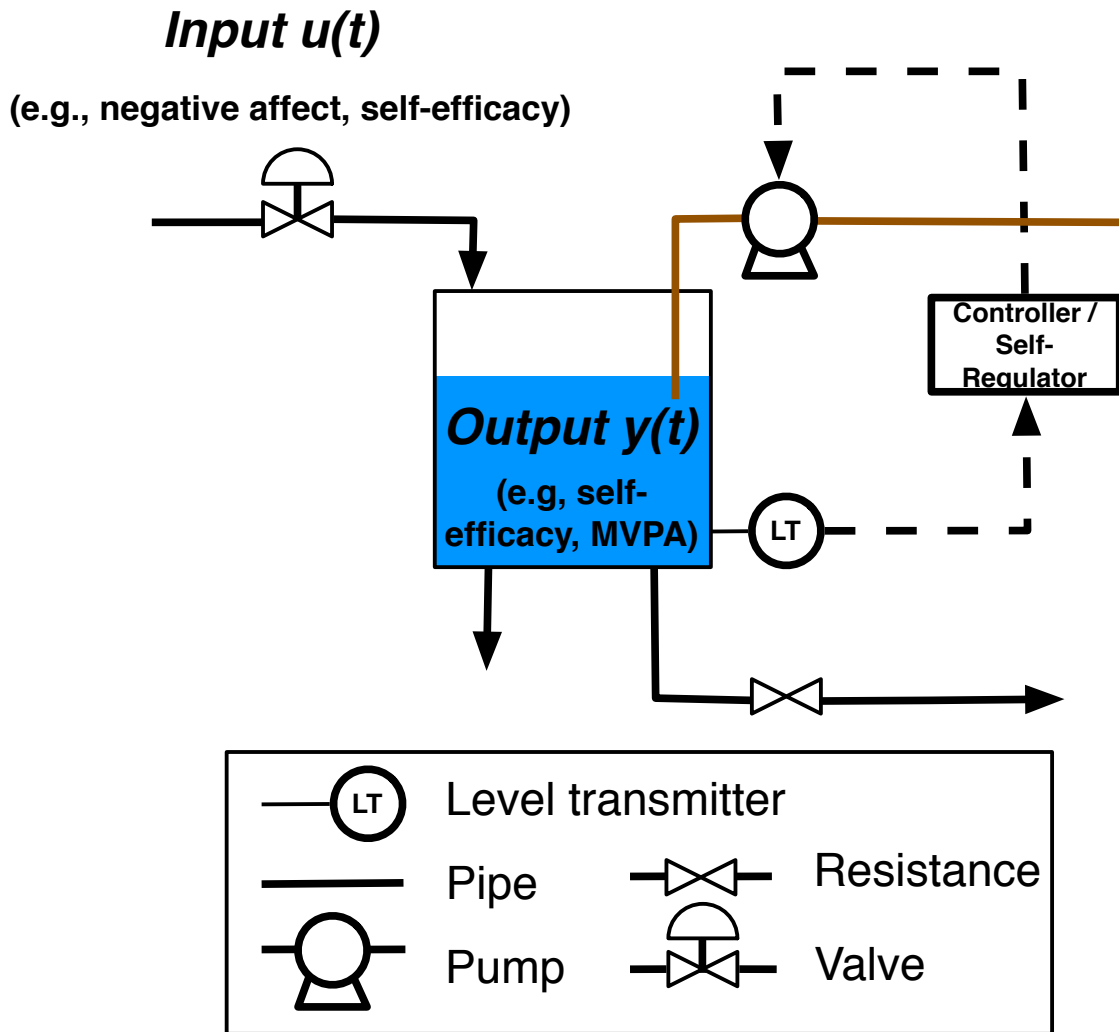


Figure 18. Fluid Analogy for Behavioral Self-Regulation

Chapter 3

SEMI-PHYSICAL MODELING OF BEHAVIORAL SYSTEM IN SINGLE-BOUT PHYSICAL ACTIVITY

3.1 Overview

In this second study, semi-physical modeling was used to identify and characterize a dynamic system relating how physical activity influences behavioral constructs and states after a bout of exercise is completed. Unlike the previous case study, this time the intensity of physical exercise is used as the driving force for the process - similar to a single bout of behavioral intervention.

The experiment was performed at UT Austin at the Environmental and Autonomic Physiology Lab. Data from a total of 45 participants was collected and used for system identification. Each participant realized a single bout of physical activity with varying levels of intensity during the process, for a total duration of 42 minutes average (with standard deviation of 2.2 minutes). During certain time intervals, spread throughout the activity, participants would respond to questions about behavioral states, generating time series for these constructs; these are dubbed the infrequent measures (when compared to the time scale of the other time series). For this experiment, the constructs measured were:

- The stage of physical activity (hereby called only Stage), that is, the exercise intensity. For this experiment, Stage assumed discrete values of 0 (sitting/resting), 2.5, 3.5, and 5.5, with the numbers representing the pace (mph) of walking.

- Heart rate (HR) measurement, collected each 30 seconds through a heart rate monitoring device (polar).

- Respiratory exchange ratio (RER) collected almost continuously when compared to the time scale of the experiment (averaged sampling time of 0.25 minute).

- Rating of perceived exertion (RPE), a behavioral construct indicating the participant's perception of his or her exertion caused by the activity. Was measured based on the Borg exertion scale, which vary from 6 (no exertion at all) to 20 (maximum exertion) (Borg, 1982). RPE was one of the more infrequent measures.

- Felt Arousal Scale (FAS), varying from 1 (low energy) to 6 (highly energized), which was also one of the infrequent time series.

- Feeling Scale (FS), varying from -5 (very bad) to +5 (very good), with 0 meaning neutral. Also one of the infrequent measures.

FAS and FS were measured and analysed under the circumplex dimensional model of affect, which considers that these two constructs combine to determine the person's basic affect state (Russel, 1978, 1980).

As well as these time series, each participant was asked to report a feeling of Pride after the exercise ("I finished with a sense of pride") on a scale ranging from 1 (Strongly Disagree) to 5 (Strongly Agree). Unlike the other measurements, Pride was not generated as a time series, instead used as a single scalar value.

The main purpose of this study was to analyse the dynamic interactions between these behavioral constructs, as well as the sensation of pride, resulting from this single bout of exercise for the participants. This analysis was performed with semi-physical identification, that is, an internal model structure was assumed, and parameter estimation followed from that theoretical model knowledge. In this case, Stage was considered to be (at first) the only exogenous input, ultimately driving all the other

behavioral signals, since the intensity of physical exercise was directly manipulated by the researchers. All the other signals were treated as outputs, although internal inter-relations between these were taken into account, since grey-box modeling allow for identification of complex sets of equations.

Based on the ideas of Ekkekakis (2003) and discussions with the investigators who collected the data, the following path diagram was initially proposed to serve as the basis of the identification study.

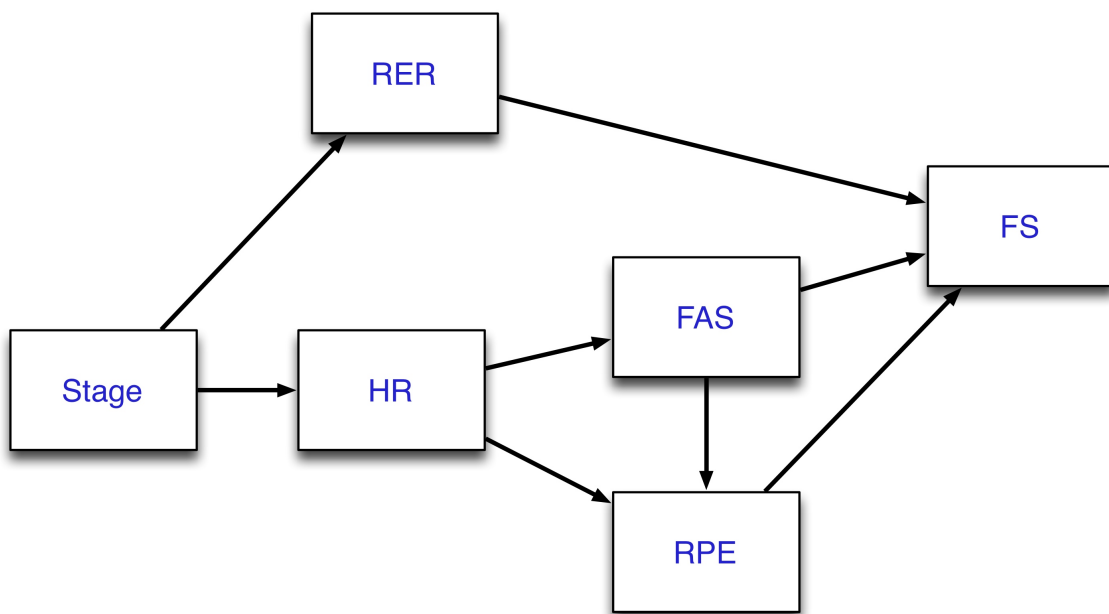


Figure 19. Initially Proposed Path Diagram for Single Exercise Bout

The diagram in Figure 19 was used as a first attempt for obtaining a mathematical model, but it does not necessarily represent the true system. Some representatives results using that diagram will be shown later. After further investigations and discussions, an alternative path diagram was used.

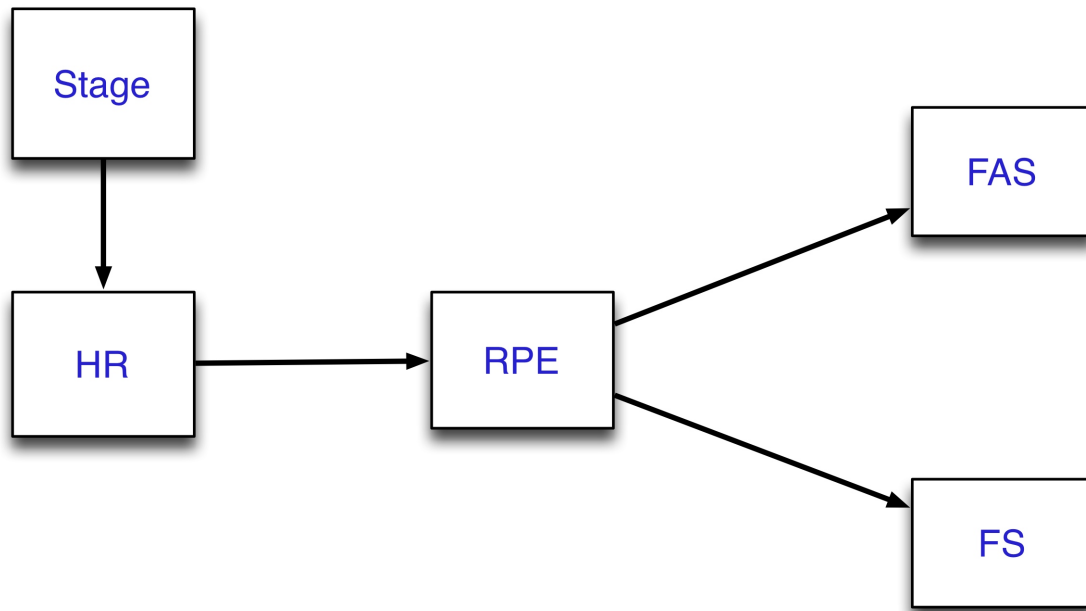


Figure 20. Proposed Path Diagram for Single Exercise Bout

This new diagram (in Figure 20) was used as the basis of the internal model needed for the grey-box routines. The direct interconnection between FAS and FS was removed to account for the bidimensional circumplex model of emotion. In this model, emotional state can be represented as a point in a two-dimensional circular space, with arousal (measured by FAS) being the vertical axis, and valence (measured by FS) being the horizontal axis (Ekkekakis, 2003; Russel, 1978, 1980). Because this model states that these constructs are independent of each other, the aforementioned variable relationship (FAS to FS) was removed in the updated diagram.

Also, the second path diagram (Figure 20) does not have a RER construct. It was speculated that RER and HR might have similar roles in influencing the behavioral variables; so, for the sake of model simplicity and parsimony, that construct was removed.

3.2 Data Analysis and Pre-Treatment

All participant data was organized in time series form containing the construct measurements (Stage, HR, RER, FAS, RPE, and FS), using the `iddata` command in MATLAB. For identification purposes, it is important that all the time series contain the same number of measurements and sampling time; however, the experimental data comprised of some frequently-measured signals (the behavioral and physiological constructs variables - Stage, HR and RER) and some signals with very few measurements in comparison (the psychological constructs measurement - FAS, RPE and FS). For this reason, the first treatment done to the data before identification was carried out was bringing all the time series to the same scale and number of data points.

Thus, the infrequent measurements (psychological signals) were linearly interpolated in order to bring these time series to the same scale as the frequent measurements. For each participant, however, psychological variable signals formed non-smooth time series with probable aliasing problems (as in, the time series values between the original data points might not be the best description of the actual pattern of the signal), and probably aliasing problems were present in the signal. This can be illustrated in Figure 21 below, which show the input-output time series (after linear interpolation) for a representative participant (Participant 2, who finished with a Sense of Pride equal to 3).

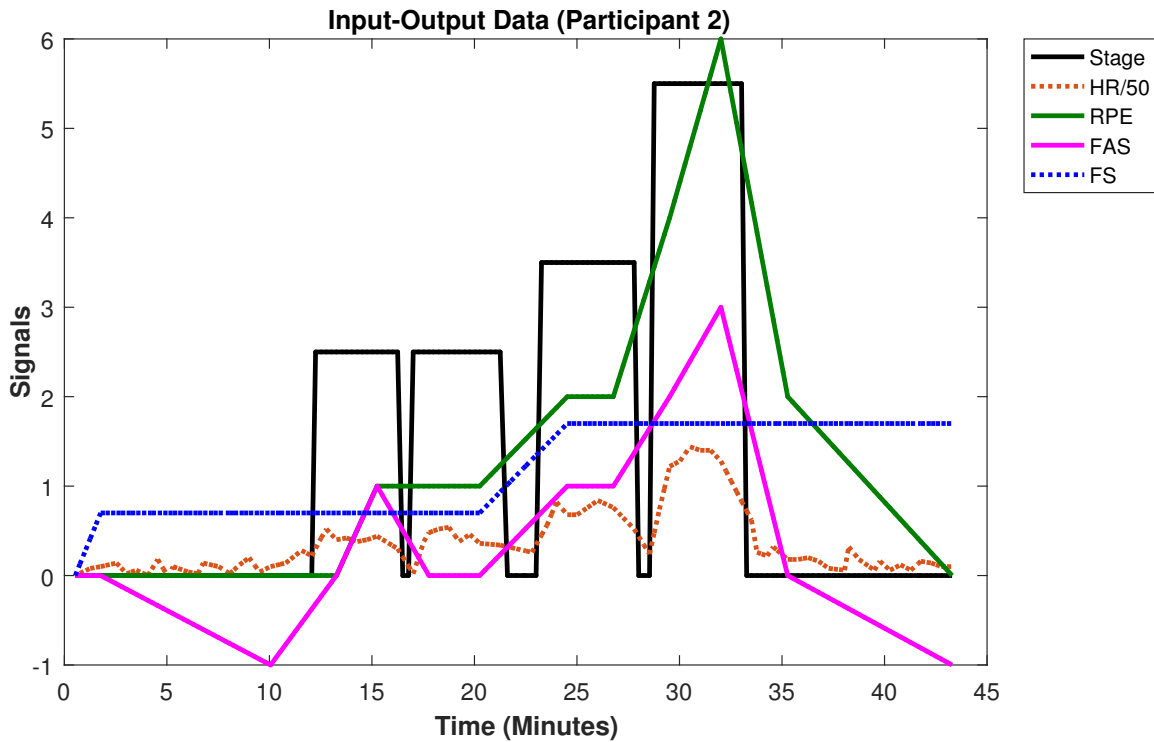


Figure 21. Time Series for Representative Participant after Linear Interpolation

To avoid these problems and obtain meaningful data signals, it was decided to average the data by splitting the participants into cohorts. Since one of the purposes of this study is to analyse the feeling of Pride after the exercise for each participant, this scalar measure was used to distinguish the three cohorts: those with reported pride equal to or lower than 3 (16 participants), those with pride equal to 4 (16 participants), and those who reported pride equal to 5 (10 participants). In each of these cohorts, all participant data was averaged so that the signals were more representative of an actual dynamic for these psychological constructs.

Some participants have more data points than others; in order to average properly and allow for easier identification, all participant's time series were clamped to a single final value (chosen to be 40 minutes); otherwise, after this time point, the averaging

become less efficient due to the lower number of participants, and thus the signals present non-smooth shapes after that point in time.

Finally, some of the output signals presented an initial slope before the input had any change (before the experiment actually begins), which was considered a side effect of the data averaging. These initial slopes were turned into stationary lines, such as seen in Figure 22. This brought the signal to a baseline level where changes would only occur after the input was excited, making for a better representation of the actual system's dynamics.

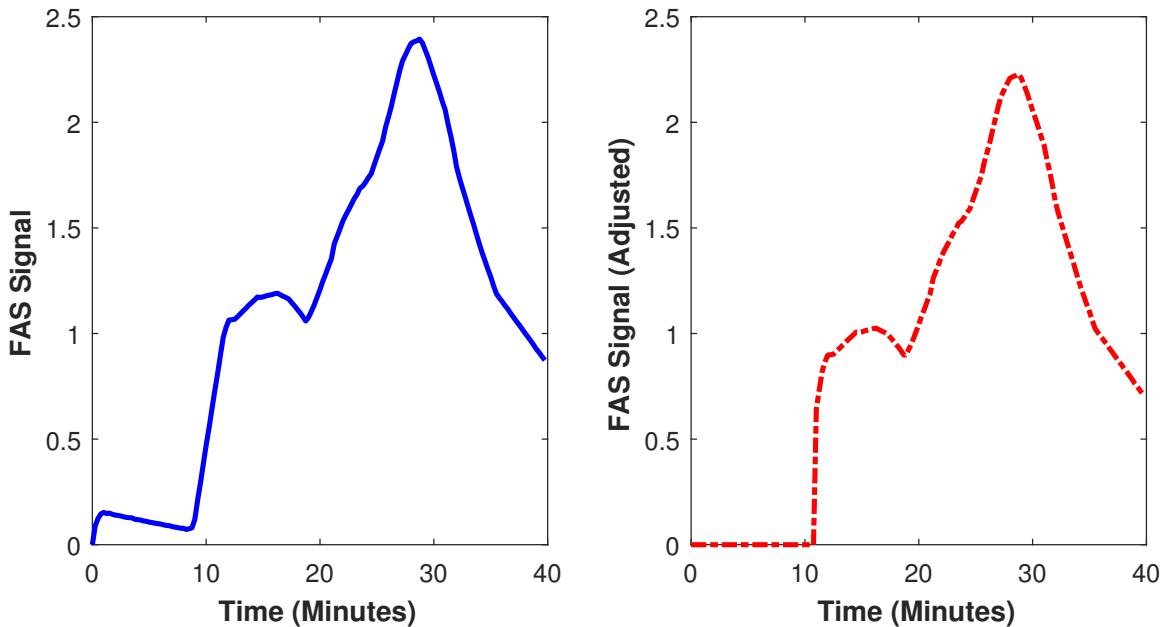


Figure 22. FAS Signal for Third Cohort Before (Left) and After (Right) Pre-Treatment

After all these steps, the experimental time series data for the three cohorts, as well as a plot showing the signals averaged over all participants for comparison, are shown below.

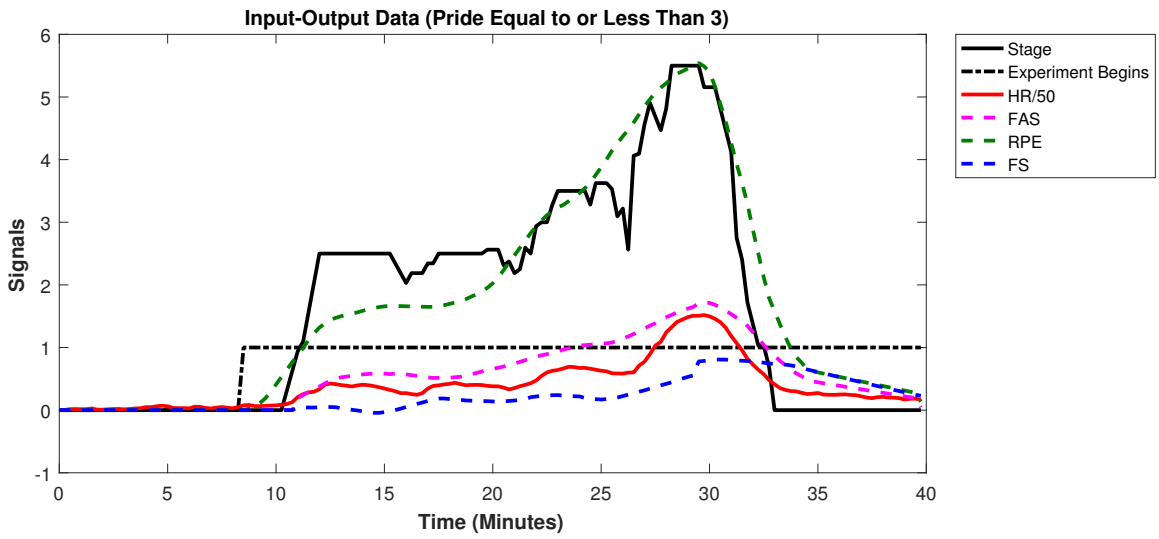


Figure 23. Time Series for Participants with Reported Pride ≤ 3

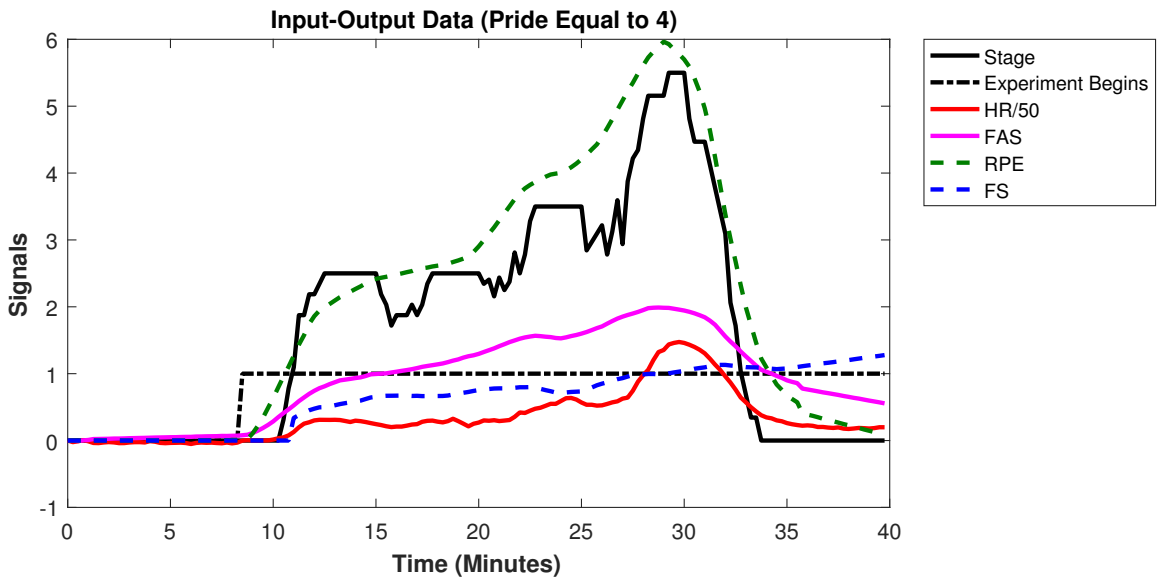


Figure 24. Time Series for Participants with Reported Pride = 4

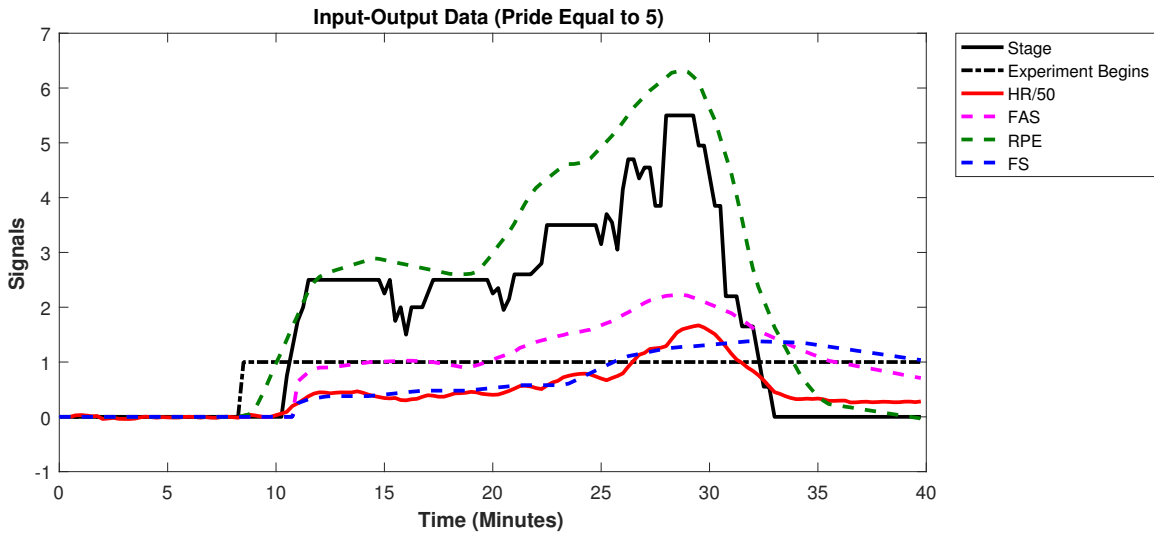


Figure 25. Time Series for Participants with Reported Pride = 5

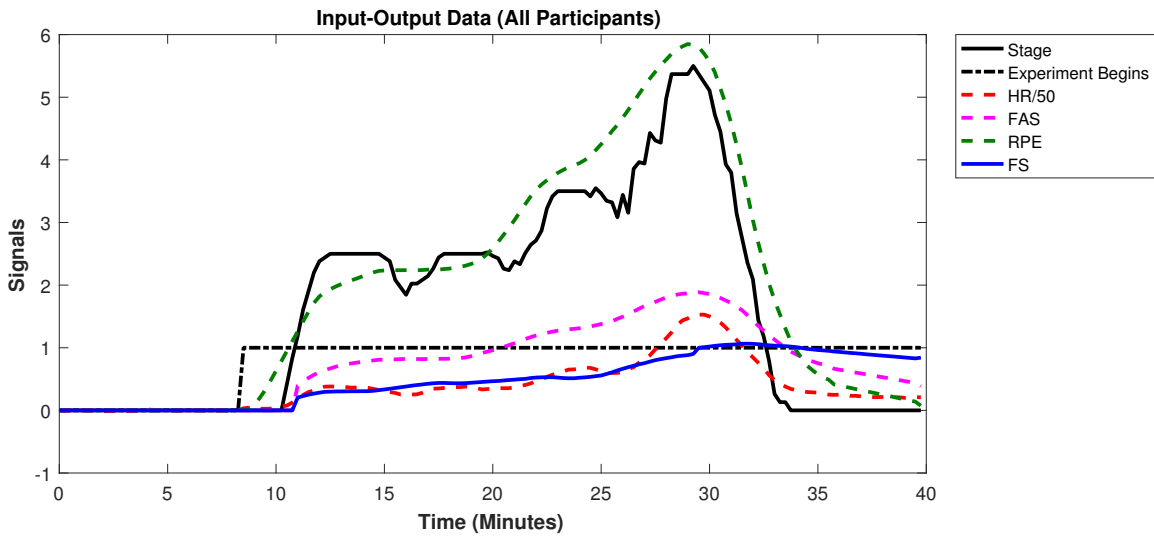


Figure 26. Time Series for All Participants

Figures 23 to 26 show the input-output signals used in the identification, that is, time series for Stage, HR, FAS, RPE, and FS after all the pre-treatment described previously. Besides the original input (Stage), there is also an exogenous input added in the system, shown in these Figures, called "Experiment Begins". The plots show

that RPE signal starts to increase before Stage increase, meaning RPE increases even before any actual physical activity is performed. For that reason, it was speculated that another input would be responsible for this early change in RPE. That is the reason for the addition of the exogenous signal "Experiment Begins", included as a unit step input - with a value changing from 0 to 1 - to represent and try to model the psychological effects that the mere knowledge of the experiment has on the behavioral variables, even before the participant starts doing physical activity. The knowledge that the experiment will begin might produce an anticipatory stress response that induces cardiovascular changes (Everson *et al.*, 1996). During the model validation phases, the addition of this new exogenous input actually improved models goodness-of-fit.

The revised path diagram that takes this new input in consideration is seen below.

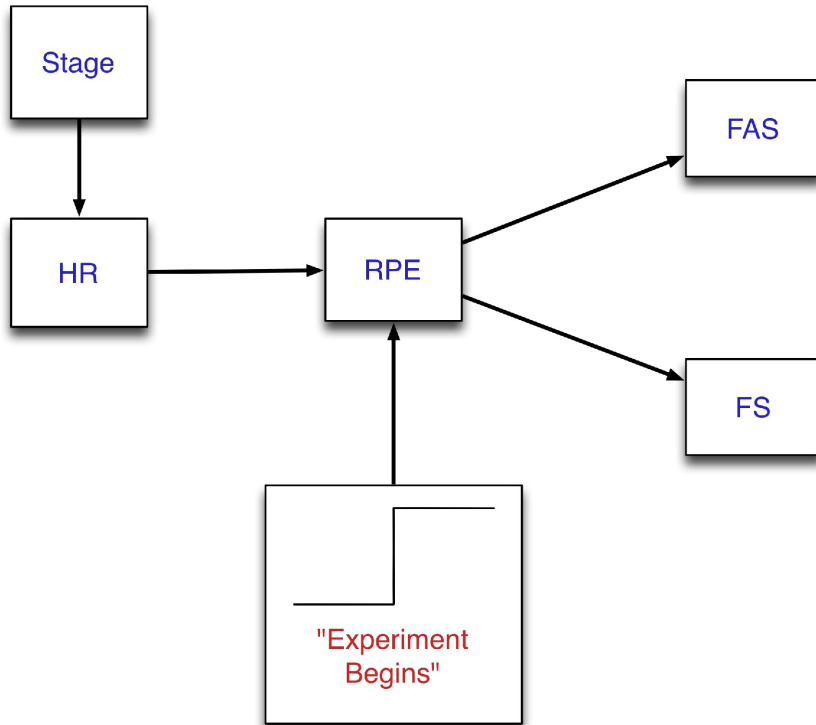


Figure 27. Revised Path Diagram with Addition of "Experiment Begins" Exogenous Input

Some general comments regarding the raw data plots (Figures 23 to 26) follow. Firstly, it is a common trend in all of the time series that most signals follow similar patterns as the Stage signal - that is, they increase and decrease in a similar fashion as the main input does. This indicates a direct dynamic relation between these constructs and the intensity of physical activity, as described in the model. The only construct which does not seem to follow the input as closely is FS. This might indicate more complex dynamics surrounding that behavioral construct.

For participants with lower self-reported feeling of pride after the exercise (Figure 23), the FS signal rapidly decreases to 0 after the activity ends (Stage signal returns to 0). In contrast, the FS signal for the other cohorts (higher sense of pride), as

well as the same signal for the plot with all participants, have a very small inclination at the end, which mean that these participants have a better ability to maintain their FS level after the activity ends. Figure 24 show a small positive inclination for the FS function, while Figures 25 and 26 show a small negative inclination. This difference between the second cohort (participants with reported pride equal to 4) and the third (reported pride equal to 5) might be due to errors due to interpolation issues; however, both cohorts show a better ability to maintain their FS after the exercise. This suggests a direct relation between the feeling of pride and the FS measurement, meaning that those with higher sense of pride are able to maintain their increased feeling affect for longer periods after the activity is done.

It is also worth mentioning that the actual magnitudes of the FS signal are different for each cohorts, with a direct relation to the reported feeling of pride. The first cohort show maximum FS values around approximately 0.8 on the scale; the second cohort, 1; and the third cohort, 1.5 (remembering that these are deviation variables, meaning that these numbers are in relation to the initial FS value prior to the activity).

Lastly, one interesting aspect to notice is how the signals for all participants in Figure 26 look "smoother" than the others. This is because that plot shows the data for the averaged signals of all participants, which thus naturally presents a better averaging than the other plots (which show the signal for each cohort).

3.3 Fluid Analogy and Mathematical Representation

From the path diagram obtained in Section 3.2 (Figure 27), a fluid analogy, as described in Section 1.6, was derived in order to obtain a mathematical description of the system in terms of differential equations.

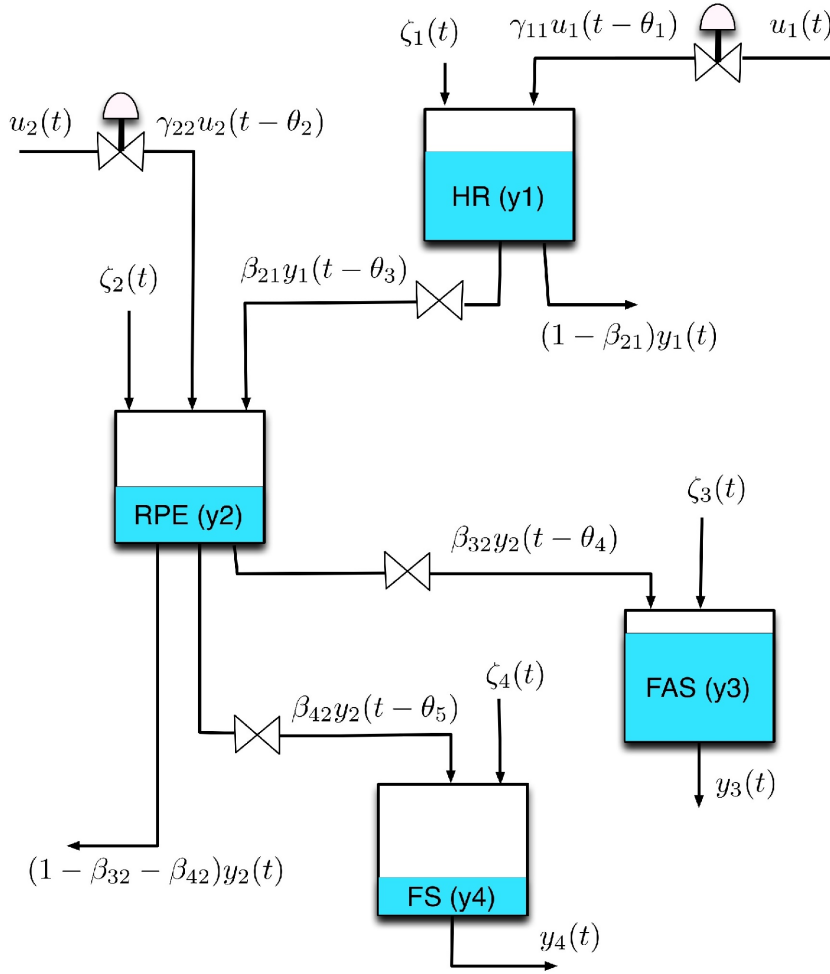


Figure 28. Fluid Analogy for the Proposed Behavioral Diagram Path

In Figure 28, u_i and y_i represent the levels of the input and output signals, respectively, as denoted in Table 4. The other notations remain similar to those used in Figure 2 - γ_{ij} for inflow resistances, β_{ij} for outflow resistances, θ_i for time delays, and ζ_i for a zero-mean stochastic signal. Although not explicitly represented in the inventory-tank depiction above, another property of the system is τ_i , the time constant associated with inventory i , which influences the speed in which the inventory's level increases or decreases.

Table 4. Notation for Input and Output Signals in Fluid Analogy for Studied Behavioral System

Notation	Signal
u_1	Stage
u_2	"Experiment Begins"
y_1	HR
y_2	RPE
y_3	FAS
y_4	FS

From this fluid analogy, material balances (Equation 1.12) were performed for each inventory. For the sake of modelling simplicity, time delays and the stochastic signals are considered to be zero ($\theta_i = \zeta_i = 0 \forall i \in [1, 2, 3, 4]$). With these simplifications, the set of differential equations obtained is:

$$\tau_1 \frac{dy_1}{dt} + y_1(t) = \gamma_{11} u_1(t) \quad (3.1)$$

$$\tau_2 \frac{dy_2}{dt} + y_2(t) = \gamma_{22} u_2(t) + \beta_{21} y_1(t) \quad (3.2)$$

$$\tau_3 \frac{dy_3}{dt} + y_3(t) = \beta_{32} y_2(t) \quad (3.3)$$

$$\tau_4 \frac{dy_4}{dt} + y_4(t) = \beta_{42} y_2(t) \quad (3.4)$$

In Equations 3.1 to 3.4, u_i and y_i are the input and output signals (as denoted in Table 4) obtained through the experimental data. The parameters that need to be identified - the core goal of this semi-physical identification procedure - are γ_{ij} , β_{ij} , and τ_i .

It is worth noting that system identification, particularly semi-physical modeling, is an iterative procedure. Even though Equations 3.1 to 3.4 were obtained through a

mathematical transcription of the behavioral path diagram, modifications to these equations (e.g., making some of the equations second order, or adding a zero) were done in order to pursue higher validation fits. Upon many re-iterations of the equations in order to pursue best goodness-of-fits and/or shape of responses, the system of equations that was found to best described the model (once again, considering time delays and stochastic signals as 0 for the sake of simplicity) was:

$$\tau_1 \frac{dy_1}{dt} + y_1(t) = \gamma_{11} \left(u_1(t) + \alpha_{11} \frac{du_1}{dt} \right) \quad (3.5)$$

$$\tau_2 \frac{dy_2}{dt} + y_2(t) = \gamma_{22} u_2(t) + \beta_{21} \left(y_1(t) + \alpha_{21} \frac{dy_1}{dt} \right) \quad (3.6)$$

$$\tau_3 \frac{dy_3}{dt} + y_3(t) = \beta_{32} y_2(t) \quad (3.7)$$

$$\tau_4^2 \frac{d^2 y_4}{dt^2} + 2\zeta_4 \tau_4 \frac{dy_4}{dt} + y_4(t) = \beta_{42} \left(y_2(t) + \alpha_{42} \frac{dy_2}{dt} \right) \quad (3.8)$$

The main differences to the first attempt (Equations 3.1 to 3.4) were the addition of the input derivatives (on the right-side of the equations) for y_1 , y_2 and y_4 equations (the terms associated with α_{11} , α_{21} , and α_{42} , respectively) and turning Equation 3.4 into a second-order differential equation (Equation 3.8). The α_{ij} terms are called the zeros of the systems, while ζ_4 is the damping coefficient, which governs the oscillation or smoothness of the second-order system (Ogunnaike and Ray, 1994). The addition of zeros allow for easier tuning of the parameters, which provides greater flexibility when adjusting parameters in order to pursue improved quality models.

From the fluid analogy, a second-order system represents a self-regulatory process (Martín Moreno, 2016), such as seen in Figure 18. The lead-lag systems (first-order

equations with input derivative) can be thought of as second order systems with a zero that dominates over one of the poles.

3.4 Grey-Box Modeling

Many different software exist that are capable of performing grey-box identification (Bohlin, 2006; Palmkvist, 2014; Sorlie, 1996). In this thesis, MATLAB's System Identification Toolbox was used. This MATLAB toolbox provides two commands necessary for the identification: `idgrey` (MathWorks, 2016c), which is used to generate a specific object type to be used by the estimation computations, and `greyest` (MathWorks, 2016b), which is the model identification *per se*. A summarized way to explain these codes is stating that the former command creates the template of the differential equations that define the system, stating which parameters are ready to be identified (free) and which are already pre-determined (fixed), while the latter command performs the parametric estimation. Important to note is that these commands are for linear systems identification; nonlinear systems must be identified with more advanced programming.

The `idgrey` command requires the user to specify the system's differential equations in state-space representation. State-space is a way of representing a system of differential equations in a compact form using matrices for states, inputs, outputs, and parameters. For linear time-invariant systems, considering deviation variables (initial, baseline values equal to 0) the representation is:

$$\begin{aligned} f = \dot{x} &= Ax + Bu + Kd \\ g = y &= Cx + Du + d \end{aligned} \tag{3.9}$$

Where f and g are vector-valued functions, x is a vector of *state variables*, u is the input vector, d is the disturbance vector, and y is the output vector. State variables are related to accumulation terms in non-stationary differential equations, and must be defined based on the equations. The state vector relates to, but is not necessarily equal to, the number of delayed inputs and outputs in the system (Rowell, 2002; Rivera, 2004).

The state-space representation is inserted into MATLAB coding by the creation of a function that relates the matrices A , B , C and D (and K and initial state vector x_0 , if needed) to the system parameters that compose them. This function is used with the `idgrey` command, as well as the actual list of parameters and their possible ranges and constraints, to create the initial setup of the model - which is an `idgrey` data object. This also includes a list of initial values for the parameters, provided by the user, which can also interfere in the way the programming takes place.

Lastly, the `greyest` command takes the `idgrey` object and the set of input-output data to perform the estimation. The result is a set of parameters that makes up the state-space matrices for the dynamic system and the simulated output response for the provided experimental input based on the identified model.

The first step in using this toolbox was to, as mentioned, write the system's equations in state-space form - that is, applying Equations 3.9 to Equations 3.5 to 3.8. The state-space matrices A , B , C , and D are defined in terms of the states, inputs, and outputs vectors by the following relations (Rivera, 2004; Rowell, 2002):

$$\begin{aligned} A &= \nabla_x \bar{f} & B &= \nabla_u \bar{f} \\ C &= \nabla_x \bar{g} & D &= \nabla_u \bar{g} \end{aligned} \tag{3.10}$$

Where

$$\nabla_z \bar{f} = \begin{bmatrix} \frac{\partial f_1}{\partial z_1} |_{\bar{x}, \bar{u}} & \cdots & \frac{\partial f_1}{\partial z_n} |_{\bar{x}, \bar{u}} \\ \vdots & \ddots & \vdots \\ \frac{\partial f_{n_f}}{\partial z_1} |_{\bar{x}, \bar{u}} & \cdots & \frac{\partial f_{n_f}}{\partial z_n} |_{\bar{x}, \bar{u}} \end{bmatrix} \quad \nabla_z \bar{g} = \begin{bmatrix} \frac{\partial g_1}{\partial z_1} |_{\bar{x}, \bar{u}} & \cdots & \frac{\partial g_1}{\partial z_n} |_{\bar{x}, \bar{u}} \\ \vdots & \ddots & \vdots \\ \frac{\partial g_{n_g}}{\partial z_1} |_{\bar{x}, \bar{u}} & \cdots & \frac{\partial g_{n_g}}{\partial z_n} |_{\bar{x}, \bar{u}} \end{bmatrix} \quad (3.11)$$

Remembering that $f = \frac{dx}{dt}$ and $g = y$. In this notation, z can be either x or u (for the sake of simplicity, disturbances and manipulated inputs can be included in the same vector u); $n = \dim(z)$, $n_f = \dim(f)$, and $n_g = \dim(g)$. Also, for the simple case of all differential equations being first order, the state vector and output vector are the same ($x = y$).

When a system has zeros (such as the case of Equation 3.5), determining the state vector is not as apparent as the regular case of systems without zeros. The procedure involves defining the states in order to find one equation for the derivative of each state \dot{x}_i relating these to each state x_i (vector f) and each input u_i , and one equation for each output y_i (vector g) again relating these to each state and each input. For the studied case, the states were defined as follow:

$$\begin{aligned} x_1 &= y_1 - \frac{\alpha_{11}\gamma_{11}}{\tau_1} u_1 \\ x_2 &= y_2 - \frac{\alpha_{21}\beta_{21}}{\tau_2} y_1 \\ x_3 &= y_3 \\ x_4 &= y_4 \\ x_5 &= \frac{dy_4}{dt} - \frac{\alpha_{42}\beta_{42}}{\tau_4^2} y_2 \end{aligned} \quad (3.12)$$

Applying these concepts to Equations 3.5 to 3.8 results in:

$$A = \begin{bmatrix} a_{11} & 0 & 0 & 0 & 0 \\ a_{21} & a_{22} & 0 & 0 & 0 \\ a_{31} & a_{32} & a_{33} & 0 & 0 \\ a_{41} & a_{42} & 0 & 0 & a_{45} \\ a_{51} & a_{52} & 0 & a_{54} & a_{55} \end{bmatrix} \quad B = \begin{bmatrix} b_{11} & 0 \\ b_{21} & b_{22} \\ b_{31} & 0 \\ b_{41} & 0 \\ b_{51} & 0 \end{bmatrix} \quad (3.13)$$

$$C = \begin{bmatrix} c_{11} & 0 & 0 & 0 & 0 \\ c_{21} & c_{22} & 0 & 0 & 0 \\ 0 & 0 & c_{33} & 0 & 0 \\ 0 & 0 & 0 & c_{44} & 0 \end{bmatrix} \quad D = \begin{bmatrix} d_{11} & 0 \\ d_{21} & 0 \\ 0 & 0 \\ 0 & 0 \end{bmatrix}$$

With

$$\begin{aligned} a_{11} &= \frac{-1}{\tau_1} & a_{21} &= \left(\frac{\beta_{21}}{\tau_2} \right) \left(1 - \frac{\alpha_{21}}{\tau_2} \right) & a_{22} &= \frac{-1}{\tau_2} & a_{31} &= \frac{\beta_{32}\beta_{21}\alpha_{21}}{\tau_3\tau_2} \\ a_{32} &= \frac{\beta_{32}}{\tau_3} & a_{33} &= \frac{-1}{\tau_3} & a_{41} &= \frac{\beta_{42}\alpha_{42}\beta_{21}\alpha_{21}}{\tau_4^2\tau_2} & a_{42} &= \frac{\beta_{42}\alpha_{42}}{\tau_4^2} \\ a_{45} &= 1 & a_{51} &= \left(\frac{\beta_{42}\beta_{21}\alpha_{21}}{\tau_4^2\tau_2} \right) \left(1 - \frac{2\zeta_4\alpha_{42}}{\tau_4} \right) & a_{52} &= \left(\frac{\beta_{42}}{\tau_4^2} \right) \left(1 - \frac{2\zeta_4\alpha_{42}}{\tau_4} \right) \\ a_{54} &= \frac{-1}{\tau_4^2} & a_{55} &= \frac{-2\zeta_4}{\tau_4} \end{aligned} \quad (3.14)$$

$$\begin{aligned} b_{11} &= \left(\frac{\gamma_{11}}{\tau_1} \right) \left(1 - \frac{\alpha_{21}}{\tau_2} \right) & b_{21} &= \left(\frac{\beta_{42}\gamma_{11}\alpha_{11}}{\tau_2\tau_1} \right) \left(1 - \frac{\alpha_{21}}{\tau_2} \right) & b_{22} &= \frac{\gamma_{22}}{\tau_2} \\ b_{31} &= \frac{\beta_{32}\beta_{21}\alpha_{21}\gamma_{11}\alpha_{11}}{\tau_3\tau_2\tau_1} & b_{41} &= \frac{\beta_{42}\alpha_{42}\beta_{21}\alpha_{21}\gamma_{11}\alpha_{11}}{\tau_4^2\tau_2\tau_1} \\ b_{51} &= \left(\frac{\beta_{42}\beta_{21}\alpha_{21}\gamma_{11}\alpha_{11}}{\tau_4^2\tau_2} \right) \left(1 - \frac{2\zeta_4\alpha_{42}}{\tau_4} \right) \end{aligned} \quad (3.15)$$

$$c_{11} = 1 \quad c_{21} = \frac{\beta_{21}\alpha_{21}}{\tau_2} \quad c_{22} = 1 \quad c_{33} = 1 \quad c_{44} = 1 \quad (3.16)$$

$$d_{11} = \frac{\gamma_{11}\alpha_{11}}{\tau_1} \quad d_{21} = \frac{\beta_{21}\alpha_{21}\gamma_{11}\alpha_{11}}{\tau_2\tau_1} \quad (3.17)$$

This state-space system was used to investigate the models generated by grey-box identification. However, because of the final values for FS signals for the cohorts with pride equal to 4 and 5 having very small inclination, these cohorts were eventually modeled as an integrator system. Doing this allowed for better model qualities to be obtained. This was done by using the same equations, but with Equation 3.8 changed to:

$$\tau_4^2 \frac{d^2 y_4}{dt^2} + 2\zeta_4 \tau_4 \frac{dy_4}{dt} = \beta_{42} y_2(t) + \alpha_{42} \frac{dy_2}{dt} \quad (3.18)$$

With state-space representation being the same, except for one element: in the matrix A , the element a_{54} is 0 (instead of $\frac{-1}{\tau_4^2}$).

Lastly, parameters ranges were also defined prior to the estimation procedure. Due to the nature of these parameters, all the time constants (τ_i) and the damping coefficient ζ_4 were forced to be greater than 0, and the gain between "Experiment Begins" and RPE (γ_{22}) was also forced to be positive - since this parameter represents the initial increase in RPE signal prior to the Stage input being excited, and in the absence of a zero for the $u_2(t)$ signal, this gain must be positive - while all the other parameters could have any value. Also, due to the lack of "physical" knowledge of the system, no parameter was fixed - all were free for estimation.

Finally, the fluid analogy imposes one last restriction. From a material balance perspective, it follows that the sum of any given inventory's outflows cannot be higher than the level of that same inventory. For an arbitrary inventory j , the outflows are β_{ij} , and thus:

$$\sum_{i=1}^N \beta_{ij} y_j(t) \leq y_j(t) \implies \sum_{i=1}^N \beta_{ij} \leq 1 \quad (3.19)$$

For the studied case, Equation 3.19 implies

$$\begin{aligned} \beta_{21} &\leq 1 \\ \beta_{32} + \beta_{42} &\leq 1 \end{aligned} \quad (3.20)$$

must be satisfied. After parametric estimation, the relations in Equation 3.20 were investigated, no matter the goodness-of-fit and shape of response.

With these matrices and the set of parameters $\mathbf{par} = [\tau_1, \tau_2, \tau_3, \tau_4, \zeta_4, \gamma_{11}, \gamma_{22}, \beta_{21}, \beta_{32}, \beta_{42}, \alpha_{11}, \alpha_{21}, \alpha_{42}]$, and their ranges, the MATLAB grey-box routines performed the identification.

All the procedures of depicting the system with a fluid analogy, writing the differential equations, and then performing grey estimation in MATLAB were also done to all the path diagrams investigated, even though this whole process is only detailed for the "current" diagram used (Figure 27).

3.5 Results and Discussion

The results of the simulation for the best models obtained - considering the path diagram in Figure 27 and the system described by the state-space representation in Equation 3.13 - are shown and discussed below. Some representative simulations for the initial path diagram (Figure 19) and system of equations (Equations 3.1 to 3.4) investigated in this study are shown in Appendix B.

Figures 29, 30, and 31 compare the simulated response obtained with the model against the experimental data, for all the four outputs in question.

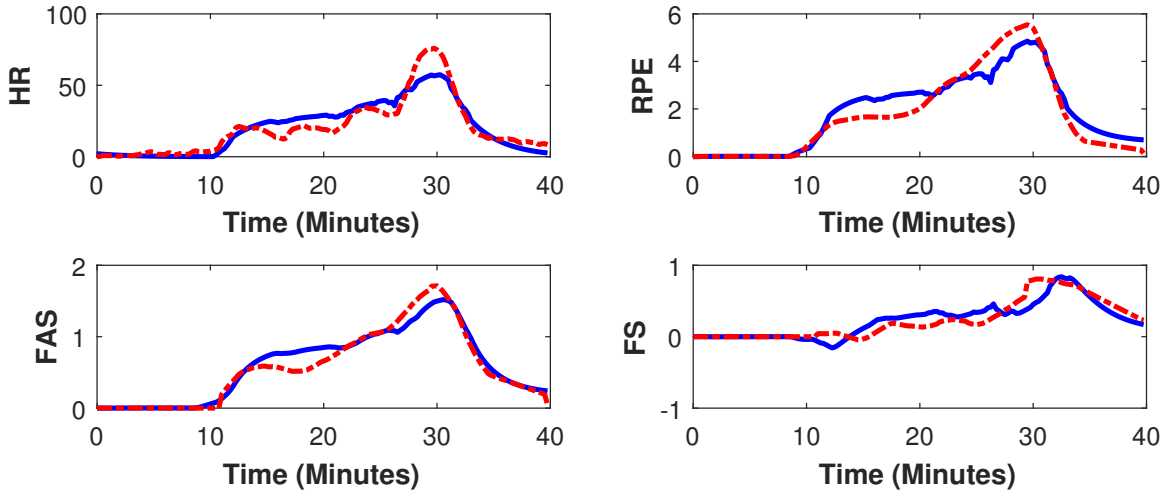


Figure 29. Simulated Outputs (Blue, Dashed) versus Experimental Outputs (Red, Dash-Dotted) for First Cohort (Pride ≤ 3).

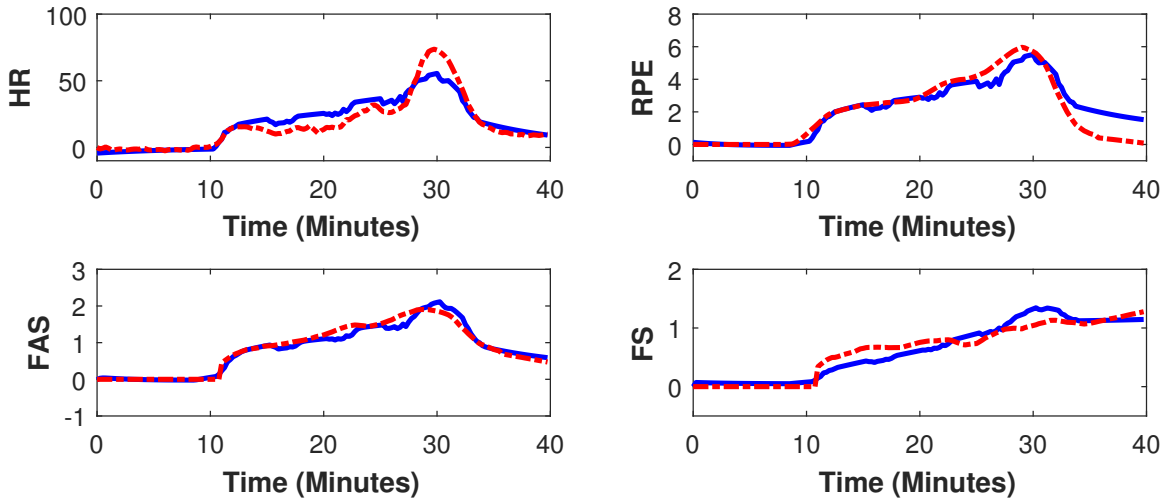


Figure 30. Simulated Outputs (Blue, Dashed) versus Experimental Outputs (Red, Dash-Dotted) for Second Cohort (Pride = 4).

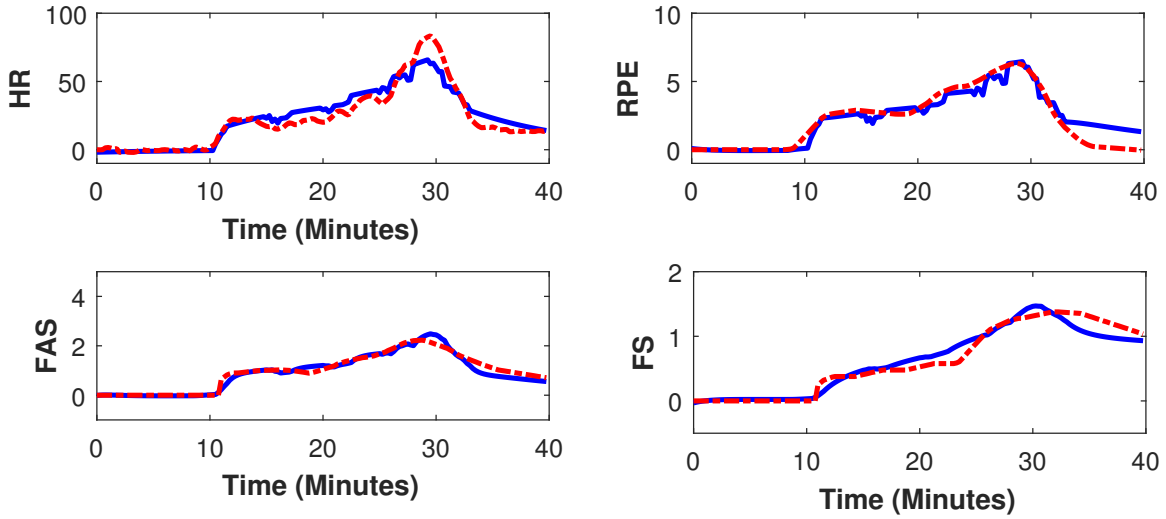


Figure 31. Simulated Outputs (Blue, Dashed) versus Experimental Outputs (Red, Dash-Dotted) for Third Cohort (Pride = 5).

Good values for fit percentage were attained by these models, as seen in Table 5.

Table 5. Goodness-of-fit for Simulated Systems for Each Cohort

Cohort	HR	RPE	FAS	FS
Pride ≤ 3	64.14%	69.59%	76.68%	53.65%
Pride = 4	62.84%	63.27%	80.46%	68.76%
Pride = 5	68.96%	67.25%	77.12%	75.83%

Goodness-of-fit were comparably similar for HR, RPE and FAS signals across the three cohorts, but significantly different for FS. This result suggests that the sense of pride reported by the participants not only influence their affective state during and after exercise (as noted previously by the fact that higher sense of pride correlate with higher FS), but is also related to model quality. The first three signals (HR, RPE, and FAS) are more tied to changes in physiology, while FS is more related to cognition / thought. It is possible that participants with lower senses of pride are more influenced by variance and the FS measurement for them more affected by measurement noises, resulting in lower model qualities; while those with higher sense of pride were able

to more accurately report their Feeling Scale and grant the model a better quality. The fact that the third cohort has fewer participants, but still a better model fit %, corroborates with this idea. However, it can also be the case that physiology predicts psychology when pride is high, but does not predict as well when pride is low. This suggests the presence of other, unmeasured predictors in the lower pride cohorts (such as frustration or disappointment).

The estimated parameters are shown in Table 6 below.

Table 6. Estimated Parameters for Semi-Physical Modeling

Parameter	Cohort 1	Cohort 2	Cohort 3
τ_1 (min)	2.98	8.21	9.49
τ_2 (min)	2	4.39	2
τ_3 (min)	0.89	0.21	0.7
τ_4 (min)	0.66	0.0005	9.78
ζ_4	1.48	22.82	2.79
γ_{11}	12.08	12.84	16.58
γ_{22}	0.6	0.76	0.27
β_{21}	0.07	0.08	0.09
β_{32}	0.32	0.38	0.4
β_{42}	0.13	0.00024	0.38
α_{11} (min)	1.01	4.11	3.73
α_{21} (min)	2.6	4.51	3
α_{42} (min)	-3.46	11.01	25.01

*Cohorts 1, 2, and 3 represent, respectively, participants with reported pride equal to 3 or lower; 4; and 5.

The list of initial parameters used in the simulations is presented in Appendix B.

The parameters τ_2 and α_{21} are, respectively, the time constant and the zero for RPE (Equation 3.6). Considering constant u_2 (for the sake of demonstration), this equation can be written in transfer function form:

$$\frac{y_2(s)}{y_1(s)} = \beta_{21} \frac{(\alpha_{21}s + 1)}{(\tau_2s + 1)} \quad (3.21)$$

Upon investigating the estimated parameters, it can be seen that, for all cohorts, α_{21} and τ_2 had similar values. This means that, in (Equation 3.21), the zero and pole almost cancel each other, making RPE (y_2) almost a scaled version of HR (y_1). In other words, the dynamics between these two constructs are very weak, almost non-existent. This is not a surprising result, since RPE scale was designed to serve as a self-reported measure of exercise intensity (Borg, 1982).

One important thing to note about the parameters in Table 6 is that the restriction imposed by Equation 3.19 are always met: β_{21} , and the sum of β_{32} with β_{42} are less than 1 for all cohorts.

The integrator action modeled for the cohorts with pride equal to 4 and 5 can be seen in these system responses. In the system described in Figure 29, FS quickly decreases when the other signal decreases. For the system shown in Figures 30 and 31, on the other hand, the experimental signal stay almost stationary after the experiment is done, which was better modeled by the integrator action. A system with integrator has the ability of maintaining the output level even after the input returns to 0. From a behavioral perspective, this means that the sense of pride indicates the participant's capacity of sustaining a change in affective state even after the physical activity ends.

A negative (right-half plane) zero was estimated for the first cohort but not for the second and third cohort. Negative zeros for second-order systems indicate an inverse response, that is, the initial direction of change is opposite to its final direction. In other words, an increase in physical activity intensity will ultimately increase the FS signal of such a participant (for the examined range of exercise intensities - higher

exercise intensities might reduce FS (Ekkekakis, 2003)), but initially it will decrease. This trend doesn't occur for participants with higher sense of pride.

Figures 32 to 35 below show the step response from each input (Stage and "Experiment Begins") to all the output signals. Because of the presence of the integrator system for the second cohort, Figure 33 shows that the time scale for the FS signal that ramps up, and thus the plot scale is not sufficient to show the dynamics for the other signals. For this reason, Figure 34 was also shown; it presents the same step responses but without the FS signal. For the cohort with highest sense of pride, the integrator is also present but was not shown in any Figure to avoid repeating information.

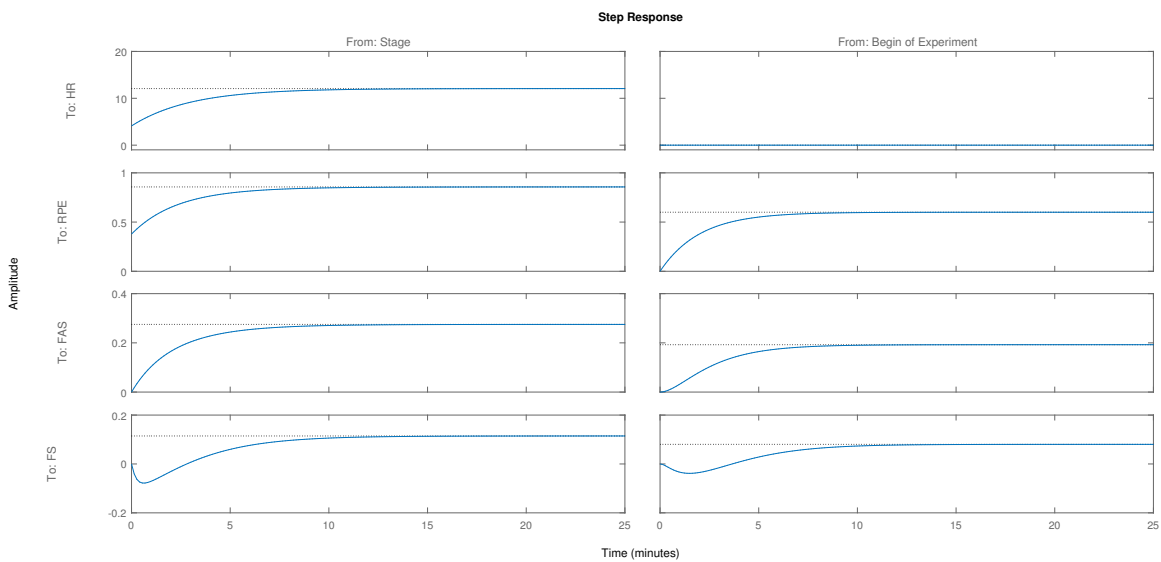


Figure 32. Unit Step Responses for First Cohort (Pride ≤ 3)

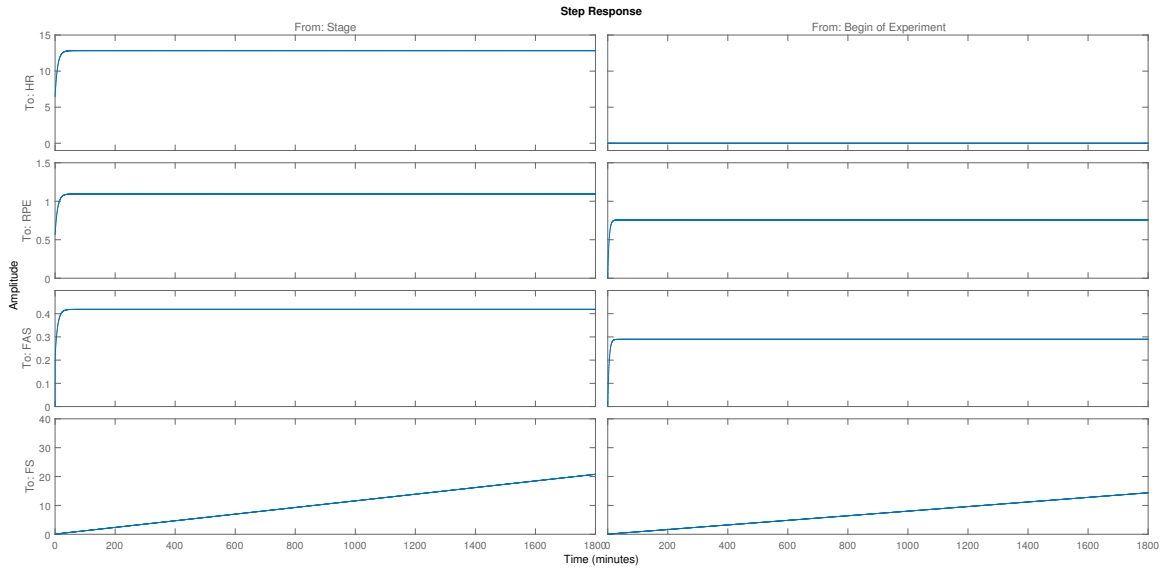


Figure 33. Unit Step Responses for Second Cohort (Pride = 4)

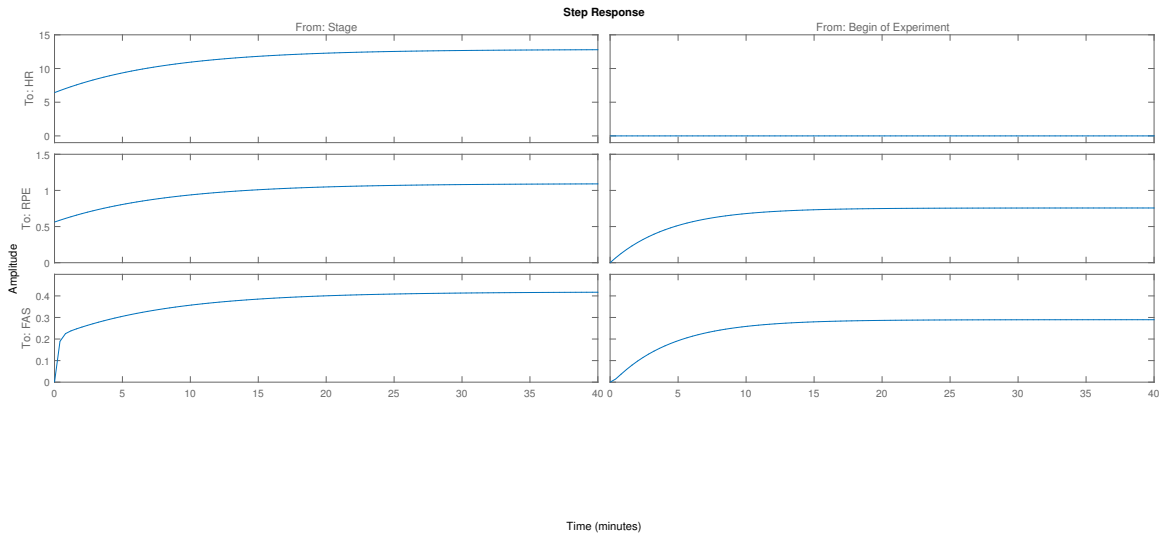


Figure 34. Unit Step Responses for Second Cohort (Pride = 4), without FS Response

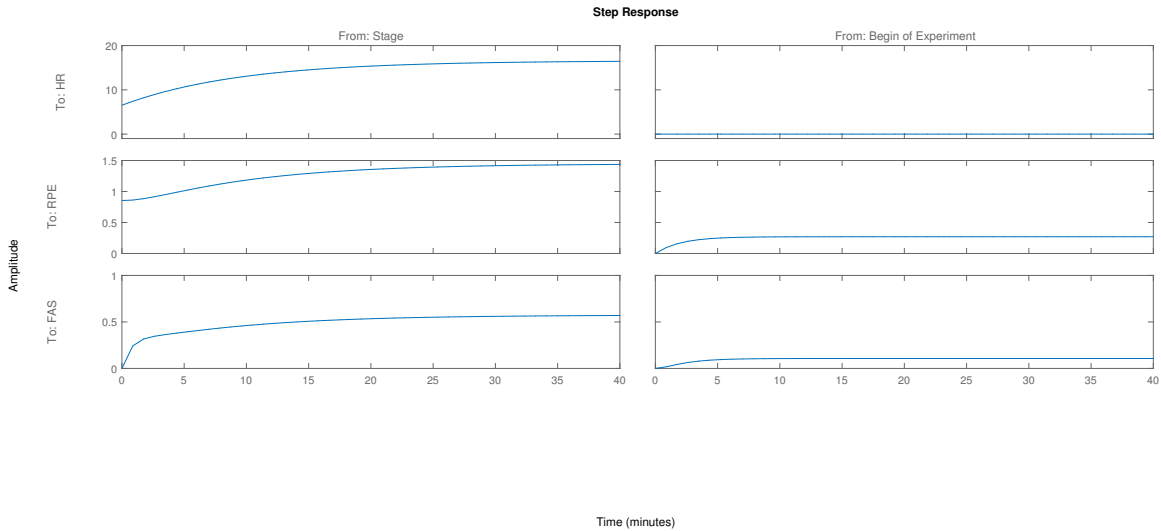


Figure 35. Unit Step Responses for Third Cohort (Pride = 5), without FS Response

Some general interpretations can be made from the step responses seen in Figures 32 to 35. The integrator action can be seen in Figure 33 by the step response from any input to FS output; instead of settling to some final value, the output signal remains increasing. If the input signal returns to 0 (representing the ending of the physical activity bout), this signal would settle in a new level, instead of also returning to 0 (which happens for systems without integrators).

The simulated model for the first cohort presents an inverse response (bottom-left plot of Figure 32), as previously characterized by the estimated left-half plane zero for that system, for the FS signal. This means that, for these participants with lowest reported sense of pride, the beginning of exercise is accompanied by an almost sudden decrease in mood affect, which then slowly recovers and reach a level higher than the baseline should the increased exercise input remain at the same level. This shape of response does not present itself to participants with higher pride; these participant benefit from increasing affect state at the start of the activity.

These responses also show that static gain between Heart Rate (HR) and the

activity intensity is higher for participants with higher pride, as seen in Table 6 (γ_{11} parameter). There are a number of implications for the use of the HR as a measure. First, it is an objective measure that is less prone to noisy measurement issues that occur with self-report measures. Second, it is measured almost immediately and is less effected by averaging or interpolation effects. Both of these indicate that HR is a more accurate measure than the others used in this simulation. Finally, HR response to exercise is an indicator of cardiorespiratory, or aerobic fitness. That is, a person is considered more aerobically fit if they can perform the same intensity of exercise with a lower HR. Because the low pride group had a lower HR response to each exercise stage, it can be inferred that they were more aerobically fit than the high pride group. This is important, because those who are less fit must work harder to complete each stage of the trial. Thus, this group responded with a greater degree of pride than the higher fit participants. The greater variability in HR for the high pride group might have provided sufficient variation to result in a better fitting model. However, it may also be that other, unmeasured cognitive factors (such as frustration, boredom, low enjoyment, etc.) might be important for the low pride group.

For these reasons, the proposed behavioral path diagram describes less fit participants better than more fit participants.

CONCLUSIONS

This study focuses on how the principles of control systems engineering, in particular system identification, can be applied to investigate and model behavioral processes during physical activities. Inter-disciplinary research involving these two fields of study is a novel way of understanding human behavior and presents the possibility of developing more efficient adaptive behavioral interventions.

The concept of fluid analogies was investigated in order to transcribe behavioral problems into a mathematical form. A behavioral path diagram describing the relations between constructs can be re-interpreted as a system of inventory and flows, and from that analogy material balances can be performed to generate a set of differential equations describing the system's dynamics. Alternatively, a dynamic model obtained through black-box identification can be analysed as a fluid system, and then re-interpreted through behavioral science concepts.

Two behavioral data sets were studied in this thesis, under the light of system identification principles. In the first case study, participant data collected through the course of four days in an observational study was used to generate black-box models relating negative affect, self-efficacy, and moderate-to-vigorous physical activity. Participants were aggregated into cohorts so that different models could describe how different types of participants behaved in the experiment. As a general result, the identification showed that the dynamic relation between negative affect and self-efficacy presents oscillatory response with negative gain, while the relation between self-efficacy and physical activity is smooth with positive gain. These results suggest the presence

of self-regulatory processes, with inefficient self-regulation for the first transfer function but more efficient for the second. This suggests that the way behavioral constructs affect actual behavior is more akin to a closed-loop system.

In the second study, physical activity intensities were prescribed to participants during single-bouts acute exercise studies while measurements of behavioral constructs were made. Through the use of fluid analogies, these experimental data were combined with a mathematical description of the model in order to estimate parameters using semi-physical identification ideas. For this study, the physical activity was the main input while physiological constructs like Heart Rate (HR) and behavioral constructs like Rate of Perceived Exertion (RPE), Felt Arousal Scale (FAS) and Feeling Scale (FS) were the output signals. Again, participants were aggregated into different cohorts so that comparisons could be made between them. A direct relation between a sense of pride reported after the exercise and the positive feeling of the participant was found, in the way that higher pride maned higher measurements of FS and also the ability of maintaining the positive feeling even after the exercise ended. The dynamic relations between activity and behavioral constructs was also found to have the influence of self-regulation.

More informative results were obtained in the first study when participants were divided by BMI Category, while participant cohort division also represented fitness level in the second study. These results suggests that participant's BMI and/or fitness level are a characteristic that influences the behavioral processes involving physical activity.

4.1 Future Work

System identification is not a procedure that can be performed once and then be concluded. Due to the very nature of this field of study, many different methods of approaching an identification problem allows for continuing investigations of the studied systems and parameters. Model structures, numerical search methods, and decisions upon which data to be used for estimation or validation are but a small number of options that can bear influence upon the dynamical system identification.

A further study that can be performed involves treating the systems as non-linear. For the sake of programming and modeling simplicity, all the models obtained in this study treated the systems as linear; although this might be a reasonable approximation for many cases, some dynamic model might represent the true systems more closely when treated as non-linear systems - and this might be specially true for social or behavioral problems. A possible way to expand this study though is analysing how non-linear modeling principles could be applied for the experimental data sets.

Run-to-run control represents the concept of controlling processes that happen in batches, with the input manipulation or determination of one batch being dependent on the results (or outputs) of previous batches. Ideas from this type of control can be applied to modeling physical activity experiments which happens over the course of different days; results from one day might influence the inputs of prescription of following days.

The ideas presented above for improving this study involves only mathematical, computational, and/or modeling suggestions, but there are even more ways to advance this work. As with any other statistical analysis, system identification techniques are more reliable when larger data sets are obtained. The ideas presented in this

thesis can be applied to behavioral experiments containing more data points (more participants and/or experiments that last longer) in order to obtain dynamic model more statistically significant.

The size of the data set is not the only possible experimental way of obtaining data that facilitates system identification. As described by Ljung (1999), the principles of system identification can inform the user or researcher about proper ways to perform data collection in order to improve the quality of identified models. In other words, there are ways to realize a data-gathering experiment that will provide results more informative about the dynamics of the studied system - this is the field of identification experiment design. These ideas, which includes topics such as decision of input and output variables and optimal input signal design, can be the basis of new behavioral experiments aimed at obtained informative data sets.

In both studies performed in this thesis, participant data was aggregated into cohorts sharing similar characteristics, and in each cohort all participant data was averaged. These divisions were done to account for problems such as data missingness and low amount of data points (in the study in Chapter 2) or signals measured with different sampling times (in the study in Chapter3). Ideally, if a large enough data set without these problems is obtained, system identification could allow for idiographic investigations, that is, dynamically modeling how each individual participant behaves during physical activity without the need to average participant data. This approach might not only reduce averaging errors but also grant insight into how individual characteristics influences the behavioral constructs.

Finally, one way that the study can be expanded is to apply control systems principles in order to design adaptive behavioral interventions as controllers. The behavioral dynamic models obtained through system identification are useful to shed

light on processes that occur in participants during the behavior, but can also form the basis of optimized health interventions. This represents a new way of approaching interventions, which stands for a promising improvement in behavioral health.

REFERENCES

- Ahn, A. C., T. A. C. Poon and R. S. Phillips, “The clinical applications of a systems approach”, *PLoS Medicine* **3**, 7 (2006).
- Ajzen, O. and T. Madden, “Prediction of goal-directed behavior: attitudes, intentions, and perceived behavioral control”, *Journal of Experimental Social Psychology* **22**, 453–474 (1986).
- Bandura, A., *Social Foundations of Thought and Action: A Social Cognitive Theory* (Prentice-Hall, 1986).
- Bohlin, T. P., *Practical Grey-box Process Identification: Theory and Applications* (Springer London, 2006).
- Bollen, K. A., *Structural Equations with Latent Variables. Series in Probability and Mathematical Statistics* (Wiley, New York, 1989).
- Borg, G. A., “Psychophysical bases of perceived exertion”, *Medicine Science in Sports Exercise* **14**, 5, 377–381 (1982).
- Carels, R. A., O. M. Douglass, H. M. Cacciapaglia and W. H. O’Brien, “An ecological momentary assessment of relapse crises in dieting”, *Journal of Consulting and Clinical Psychology* **72**, 2, 341 (2004).
- Carver, C. S. and M. F. Scheier, *On the self-regulation of behavior* (Cambridge University Press, New York, 1998).
- Carver, C. S. and M. F. Scheier, “Control processes and self-organization as complementary principles underlying behavior”, *Personality and Social Psychology Review* **6**, 4, 304–315 (2002).
- Collins, L. M., S. A. Murphy and K. L. Bierman, “A conceptual framework for adaptive preventive interventions”, *Prevention Science* **5**, 3, 185–196 (2004).
- Davison, D. E., R. Vanderwater and K. Zhou, “A control-theory reward-based approach to behavior modification in the presence of social-norm pressure and conformity pressure”, in “Proceedings of the 2011 American Control Conference”, pp. 1861–1866 (San Francisco, USA, June 2011).
- Dong, Y., D. E. Rivera, D. S. Downs, J. S. Savage, D. M. Thomas and L. M. Collins, “Hybrid model predictive control for optimizing gestational weight gain behavioral interventions”, in “Proceedings of the 2013 American Control Conference”, pp. 1970–1975 (Washington D.C., USA, June 2013).

- Dong, Y., D. E. Rivera, D. M. Thomas, J. E. Navarro-Barrientos, D. S. Downs, J. S. Savage and L. M. Collins, “A dynamical systems model for improving gestational weight gain behavioral interventions”, in “Proceedings of the 2012 American Control Conference”, pp. 4059–4064 (Montreal, Quebec, Canada, June 2012).
- Dunton, G. F. and A. A. Atienza, “The need for time-intensive information in healthful eating and physical activity research: a timely topic”, *Journal of the American Dietetic Association* **109**, 1, 30–35 (2009).
- Dunton, G. F., A. A. Atienza, C. M. Castro and A. C. King, “Using ecological momentary assessment to examine antecedents and correlates of physical activity bouts in adult age 50+ years: a pilot study”, *Annals of Behavioral Medicine* **38**, 3, 249–255 (2009).
- Dunton, G. F., J. Huh, A. M. Leventhal, N. Riggs, D. Hedeker, D. Spruijt-Metz and M. A. Pentz, “Momentary assessment of affect, physical feeling states, and physical activity in children”, *Health Psychology* **33**, 3, 255 (2014).
- Dunton, G. F., S. S. Intille, J. Wolch and M. A. Pentz, “Children’s perceptions of physical activity environments captured through ecological momentary assessment: a validation study”, *Preventive Medicine* **55**, 2, 119–121 (2012).
- Dunton, G. F., Y. Liao, S. Intille, J. Wolch and M. A. Pentz, “Physical and social contextual influences on children’s leisure-time physical activity: an ecological momentary assessment study”, *Journal of Physical Activity and Health* **8**, Suppl 1, S103–108 (2011a).
- Dunton, G. F., Y. Liao, S. S. Intille, D. Spruijt-Metz and M. Pentz, “Investigating children’s physical activity and sedentary behavior using ecological momentary assessment with mobile phones”, **19**, 6, 1205–1212 (2011b).
- Dunton, G. F., D. E. Rivera, A. A. Atienza, R. P. Moser, E. B. Hekler and W. T. Riley, “Dynamical systems modeling of time-intensive behavioral data: An illustration from an ecological momentary assessment study of physical activity”, *Manuscript* (2015).
- Ekkekakis, P., “Pleasure and displeasure from the body: Perspectives from exercise”, *Cognition and Emotion* **17**, 2, 213–239 (2003).
- Everson, S. A., G. A. Kaplan, D. E. Goldberg and J. T. Salonen, “Anticipatory blood pressure response to exercise predicts future high blood pressure in middle-aged men”, *Hypertension* **27**, 5, 1059–1064 (1996).
- Franklin, G. F., J. D. Powell and A. Emami-Naeni, *Feedback control of dynamics systems* (Prentice Hall Inc., 2006).

- Freisthler, B., S. Lipperman-Kreda, M. Bersamin and P. J. Gruenewald, “Tracking the when, where, and with whom of alcohol use: Integrating ecological momentary assessment and geospatial data to examine risk for alcohol-related problems”, *Alcohol Research: Current Reviews* **36**, 1, 29–38 (2015).
- Froehlich, J., M. Chen, S. Consolvo, B. Harrison and J. Landay, “Myexperience: A system for in situ tracing and capturing of user feedback on mobile phones”, in “Proceedings of the 5th International Conference on Mobile Systems, Applications and Services”, (New York, NY, 2007).
- Godin, G., P. Valois and L. Lepage, “The pattern of influence of perceived behavioral control upon exercising behavior: An application of ajzen’s theory of planned behavior”, *Journal of Behavioral Medicine* **16**, 1, 81–102 (1993).
- Hauth, J., *Grey-Box Modelling for Nonlinear Systems*, Ph.D. thesis, Technische Universität Kaiserslautern [Technical University of Kaiserslautern], Kaiserslautern, Germany (December 2008).
- Heckler, E. B., P. Klansja, V. Traver and M. Hendriks, “Realizing effective behavioral management of health: the metamorphosis of behavioral science methods”, *IEEE Pulse* **4**, 5, 29–34 (2013).
- Hekler, E. B., M. P. Buman, D. Ahn, G. Dunton, A. A. Atienza and A. C. King, “Are daily fluctuations in perceived environment associated with walking?”, *Psychology and Health* **27**, 9, 1009–1020 (2012).
- Kaplan, R. M. and A. A. Stone, “Bringing the laboratory and clinic to the community: mobile technologies for health promotion and disease prevention”, *Annual Review of Psychology* **64**, 471–498 (2013).
- Ljung, L., *System Identification: Theory for the User* (Prentice Hall PTR, 1999).
- Ljung, L., “Prediction error estimation methods”, Tech. Rep. LiTH-ISY-R-2365, Department of Electrical Engineering, Linköping University, SE-581 83 Linköping, Sweden (2001).
- Locke, E. A. and G. P. Latham, *A theory of goal setting and task performance* (Prentice Hall, NJ, 1990).
- Martín Moreno, C. A., *A System Identification and Control Engineering Approach to Optimizing mHealth Behavioral Interventions Based on Social Cognitive Theory*, Ph.D. thesis, Arizona State University, Tempe, AZ (August 2016).
- MathWorks, “Loss function and model quality metrics”, <https://www.mathworks.com/help/ident/ug/model-quality-metrics.html> (2016a).

- MathWorks, “greyest matlab documentation page”, <https://www.mathworks.com/help/ident/ref/greyest.html> (2016b).
- MathWorks, “idgrey matlab documentation page”, <https://www.mathworks.com/help/ident/ref/idgrey.html> (2016c).
- Nandola, N. N. and D. E. Rivera, “An improved formulation of hybrid model predictive control with application to production-inventory systems”, *IEEE Trans. Control Systems Tech.* **21**, 1, 121–135 (2013).
- Navarro-Barrientos, J.-E., D. E. Rivera and L. M. Collins, “A dynamical model for describing behavioural interventions for weight loss and body composition change”, *Mathematical and Computer Modeling of Dynamical Systems* **17**, 2, 183–203 (2011).
- Neck, R., “Control theory and economic policy: Balance and perspectives”, *Annual Reviews in Control* **33**, 1, 79–88 (2009).
- Noar, S. M. and R. S. Zimmermann, “Health behavior theory and cumulative knowledge regarding health behaviors: are we moving in the right direction?”, *Health Education Research* **20**, 3, 275–290 (2005).
- Norman, P., M. Conner and R. Bell, “The theory of planned behaviour and exercise: Evidence for the moderating role of the past behaviour”, *British Journal of Health Psychology* **5**, 249–261 (2000).
- Ogunnaike, B. A. and W. H. Ray, *Process Dynamics, Modeling and Control* (Oxford University Press, 1994).
- Palmkvist, E., “Implementation of grey-box identification in jmodelica.org”, (2014).
- Patrick, K., W. G. Griswold, F. Raab and S. S. Intille, “Health and the mobile phone”, *American journal of preventive medicine* **35**, 2, 177–181 (2008).
- Piasecki, T. M., C. J. Trela, D. Hedeker and R. J. Mermelstein, “Smoking antecedents: Separating between-and within-person effects of tobacco dependence in a multiwave ecological momentary assessment investigation of adolescent smoking”, *Nicotine Tobacco Research* **16**, Suppl 2, S119–S126 (2014).
- Posner, J., J. A. Russell and B. S. Peterson, “The circumplex model of affect: an integrative approach to affective neuroscience, cognitive development, and psychopathology”, *Development and psychopathology* **17**, 3, 715–734 (2005).
- Riley, W. T., D. E. Rivera, A. A. Atienza, W. Nilsen, S. M. Allison and R. Mermelstein, “Health behavior models in the age of mobile interventions: are our theories up to the task?”, *Translational Behavioral Medicine* **1**, 1, 53–71 (2011).

- Rivera, D. E., “State-space models and linearization”, Handout for ChE 461 Process Dynamics and Control, School for the Engineering of Matter, Transport, and Energy, Arizona State University (2004).
- Rivera, D. E., M. D. Pew and L. M. Collins, “Using engineering control principles to inform the design of adaptive interventions: A conceptual introduction”, *Drug and Alcohol Dependence* **88**, Supplement 2, S31–S40 (2007).
- Roth, A. M., D. J. Hensel, J. D. Fortenberry, R. S. Garfein, J. K. Gunn and S. E. Wiehe, “Feasibility and acceptability of cell phone diaries to measure hiv risk behavior among female sex workers”, *AIDS and Behavior* **18**, 12, 2314–2324 (2014).
- Rowell, D., “State-space representation of lti systems”, <http://web.mit.edu/2.14/www/Handouts/StateSpace.pdf>, handout for 2.14 Analysis and Design of Feedback Control Systems, Department of Mechanical Engineering, MIT (2002).
- Russel, J. A., “Evidence of convergent validity on the dimensions of affect”, *Journal of Personality and Social Psychology* **36**, 10, 1152–1168 (1978).
- Russel, J. A., “A circumplex model of affect”, *Journal of Personality and Social Psychology* **39**, 1161–1178 (1980).
- Schroeder, S. A., “We can do better: Improving the health of the american people”, *New England Journal of Medicine* **357**, 1221–1228 (2007).
- Schwartz, J. D., W. Wang and D. E. Rivera, “Optimal tuning of process control based decision policies for inventory management in supply chains”, *Automatica* **42**, 1311–1320 (2006).
- Shiffman, C. J., S. an Gwaltney, M. H. Balabanis, K. S. Liu, J. A. Paty, J. D. Kassel and M. Gnys, “Immediate antecedents of cigarette smoking: an analysis from ecological momentary assessment”, *Journal of Abnormal Psychology* **111**, 4, 531 (2002).
- Shiffman, S., M. H. Balabanis, C. J. Gwaltney, J. A. Paty, M. Gnys, J. D. Kassel and S. M. Paton, “Prediction of lapse from associations between smoking and situational antecedents assessed by ecological momentary assessment”, *Drug and alcohol dependence* **91**, 2, 159–168 (2007).
- Shiffman, S., A. A. Stone and M. R. Hufford, “Ecological momentary assessment”, *Annual Review of Clinical Psychology* **4**, 1–32 (2008).
- Sorlie, J. A., *On Grey-Box Model Definition and Symbolic Derivation of Extended Kalman Filters*, Ph.D. thesis, Department of Signals, Sensors and Systems, Royal Institute of Technology, Sweden (1996).

- Swendsen, J., F. Serre, M. Fatseas and M. Auriacombe, “A systematic review of studies exploring craving, its moderators, and the link with substance use in daily life using ecological momentary assessment (ema)”, *Drug Alcohol Dependence* **140**, e221 (2014).
- Symons Downs, D. and H. A. Hausenblas, “The theories of reasoned action and planned behavior applied to exercise: A meta-analytic update”, *Journal of Physical Activity and Health* **2**, 76–97 (2005).
- Timms, K. P., *A Novel Engineering Approach to Modeling and Optimizing Smoking Cessation Interventions*, Ph.D. thesis, Arizona State University, Tempe, AZ (December 2014).
- Vanderwater, R. and D. E. Davison, “A dynamic control approach to studying the effectiveness of rewards in inducing behavior and attitude change”, in “Proceedings of the IEEE International Conference of Control and Automation”, pp. 1062–1067 (Christchurch, New Zealand, December 2009).
- Vanderwater, R. and D. E. Davison, “Using rewards to change a person’s behavior: a double-integrator output-feedback dynamic control approach”, in “Proceedings of the 2011 American Control Conference”, pp. 4046–4052 (Montreal, Quebec, Canada, June-July 2012).
- Wang, W. and D. E. Rivera, “Model predictive control for tactical decision-making in semiconductor manufacturing supply chain management”, *IEEE Trans. Control Systems Tech.* **16**, 5, 841–855 (2008).
- Wellstead, P., E. Bullinger, D. Kalamatianos, O. Mason and M. Verwoerd, “The role of control and system theory in systems biology”, *Annual Reviews in Control* **32**, 1, 33–47 (2008).
- Whiten, B., “Model completion and validation using inversion of grey box models”, *Australian and New Zealand Industrial and Applied Mathematics Journal* **54**, C187–C199 (2013).
- World Health Organization, “Obesity and overweight”, <http://www.who.int/mediacentre/factsheets/fs311/en/>, accessed in: October 05, 2016 (2016).

APPENDIX A

ESTIMATED ARX PARAMETERS FOR DYNAMIC SYSTEMS IDENTIFIED IN
CHAPTER 2

Tables 7 and 8 contains the parameters estimated for the identified models in Chapter 2, with the most general form of the ARX model obtained in this problem being represented by:

$$\begin{aligned}
 y(t) + a_1y(t-1) + a_2y(t-2) + a_3y(t-3) + a_4y(t-4) = \\
 = b_1u(t-1) + b_2u(t-2) + b_3u(t-3) + b_4u(t-4) + b_5u(t-5) + e(t)
 \end{aligned}
 \tag{A.1}$$

Worth noting that all the identified models had $n_k = 1$.

Table 7. Estimated ARX Parameters

System	a_1	a_2	a_3	a_4
All				
Participants				
NA to SE	-1.7	0.9359	0	0
SE to MVPA	0.2474	-0.3095	-0.2159	0
Age < Median				
NA to SE	-0.6866	-0.3787	0.5853	0.07748
SE to MVPA	0.06139	-0.00921	0.1648	0
Age > Median				
NA to SE	-1.502	1.529	-0.6809	0.2374
SE to MVPA	0.1739	-0.2124	0	0
Females				
NA to SE	-0.7861	-0.4563	-0.2092	0.6025
SE to MVPA	-0.01011	0.06601	0.04251	-0.255
Males				
NA to SE	-0.6884	-0.4555	0.6746	0
SE to MVPA	0.6836	0.152	-0.489	-0.1524
Underweight				
/ Normal				
NA to SE	-1.217	0.4223	0.2305	0
SE to MVPA	-0.2094	-0.2064	-0.4378	-0.01813
Overweight				
/ Obese				
NA to SE	-1.348	0.6351	0.1411	0
SE to MVPA	-0.8773	0.4136	-0.1364	0

Table 8. Estimated ARX Parameters (Cont.)

System	b_1	b_2	b_3	b_4	b_5
All					
Participants					
NA to SE	-1.811	0.2109	0.08771	-1.114	0.3211
SE to MVPA	-0.007612	0.8245	0.1494	0	0
Age < Median					
NA to SE	-0.398	-1.112	0	0	0
SE to MVPA	0.2216	0	0	0	0
Age > Median					
NA to SE	-1.063	-0.3994	-1.01	0	0
SE to MVPA	0.03531	0.29	0	0	0
Females					
NA to SE	-0.8539	0	0	0	0
SE to MVPA	-0.04335	0.5016	0	0	0
Males					
NA to SE	-0.1564	0.007614	-1.378	0	0
SE to MVPA	1.91	1.842	0.8771	0	0
Underweight					
/ Normal					
NA to SE	-0.3202	0	0	0	0
SE to MVPA	0.538	0	0	0	0
Overweight					
/ Obese					
NA to SE	-0.4666	1.284	-1.618	0	0
SE to MVPA	0.9679	0.4096	-0.5756	0.572	0

APPENDIX B

GREY-BOX MODELING CONSIDERATIONS FOR SYSTEMS IDENTIFIED IN

CHAPTER 3

B.1 Initial Parameters for Simulation

The table below presents the initial parameters used for simulation in each model.

Table 9. Initial Parameters for Grey-Box Simulation

Parameter	Cohort 1*	Cohort 2*	Cohort 3*
τ_1	2	2	2
τ_2	2	1	2
τ_3	2	2	2
τ_4	2	20	10
ζ_4	1	1	1
γ_{11}	10	10	10
γ_{22}	0.6	2	1
β_{21}	0.1	0.05	0.05
β_{32}	0.5	0.5	0.5
β_{42}	0.5	0.5	0.7
α_{11}	2	2	2
α_{21}	2	2	2
α_{42}	2	2	2

*Cohorts 1, 2, and 3 represent, respectively, participants with reported pride equal to 3 or lower; 4; and 5.

B.2 Representative Simulations for Investigated Diagrams and Equations

The resulting semi-physical simulation for some intermediate path diagrams that were investigated are shown, as well as the goodness-of-fit. The first simulation (Figure 37) used the diagram in Figure 19, which contains the RER construct, an interconnection between FAS and FS, and only 1 input signal.

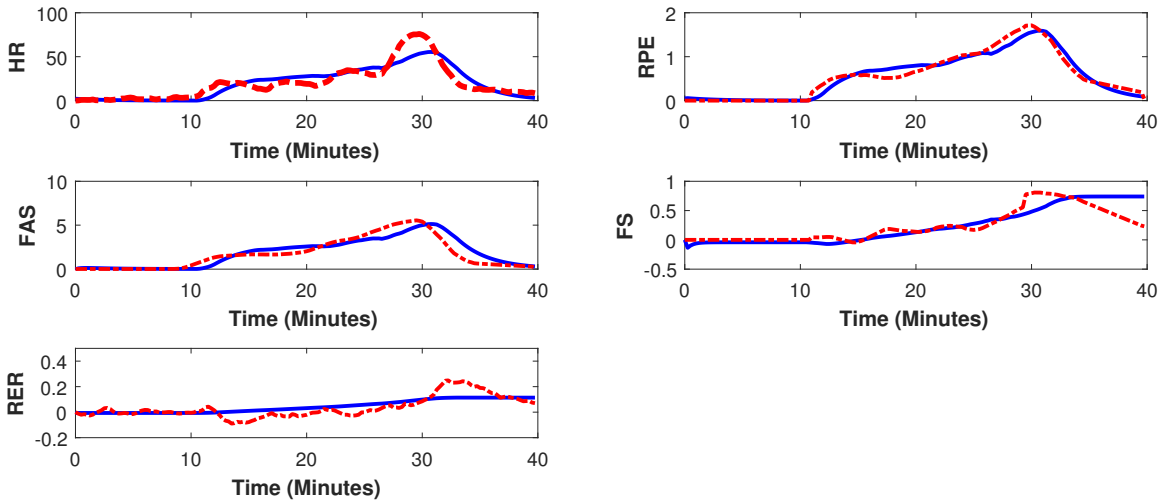


Figure 36. Simulated Outputs (Blue, Dashed) versus Experimental Outputs (Red, Dash-Dotted) for First Cohort ($Pride \leq 3$) for Diagram in Figure 18.

Using the diagram depicted in Figure 27 but with all differential equations being first order and having no zeroes (Equations 3.1 to 3.4) yield the following simulation.

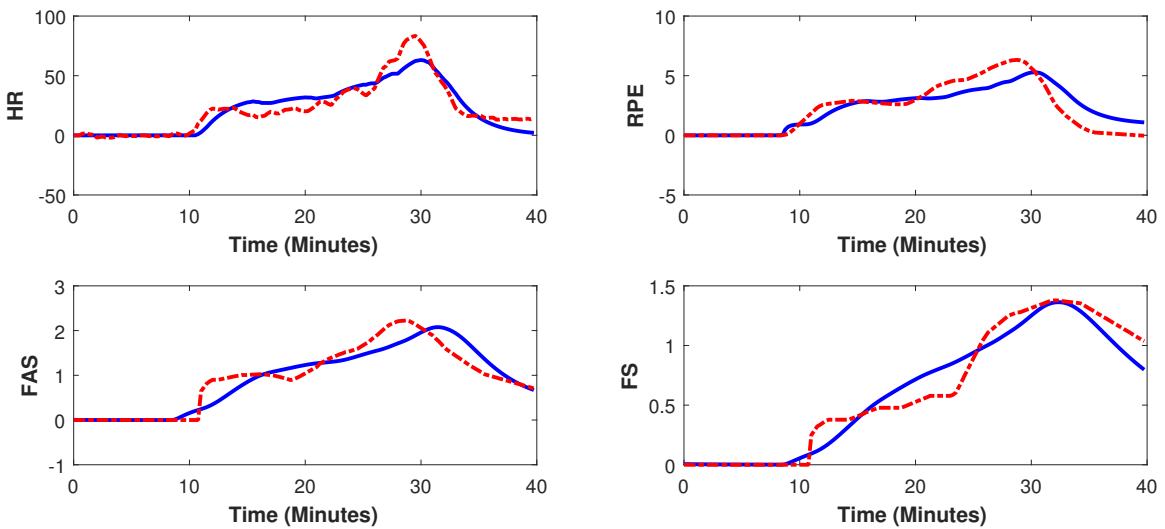


Figure 37. Simulated Outputs (Blue, Dashed) versus Experimental Outputs (Red, Dash-Dotted) for Third Cohort ($Pride = 5$) for Diagram in Figure 25.

For the two representative simulations above, the following table shows the goodness-of-fit.

Table 10. Goodness-of-fit for Representative Simulations Above

Representative Simulation	HR	RPE	FAS	FS	RER
Figure 34	56.07%	58.63%	77.75%	42.65%	36.19%
Figure 35	63.13%	52.9%	63.44%	75.95%	-